PCT

WORLD INTELLECTUAL PROPERTY ORGANIZATION
International Bureau

INTERNATIONAL APPLICATION PUBLISHED UNDER THE PATENT COOPERATION TREATY (PCT)

(51) International Patent Classification 6 : G01B 11/24	A1	(11) International Publication Number: WO 99/28704
		(43) International Publication Date: 10 June 1999 (10.06.99)

(21) International Application Number: PCT/EP98/07705

(22) International Filing Date: 30 November 1998 (30.11.98)

(30) Priority Data:
MI97A002667 2 December 1997 (02.12.97) IT

(71) Applicant *(for all designated States except US)*: UNIVERSITA' DEGLI STUDI DI BRESCIA [IT/IT]; Piazza Mercato, 15, I–25100 Brescia (IT).

(72) Inventors; and
(75) Inventors/Applicants *(for US only)*: SANSONI, Giovanna [IT/IT]; Universita' Degli Studi di Brescia, Via Branze, 38, I–25123 Brescia (IT). LAZZARI, Sara [IT/IT]; Universita' Degli Studi di Brescia, Via Branzze, 38, I–25123 Brescia (IT).

(74) Agents: TRUPIANO, Roberto et al.; Brevetti Europa S.r.l., Corso di Porta Ticinese, 3, I–20123 Milano (IT).

(81) Designated States: AU, CA, CN, JP, US, European patent (AT, BE, CH, CY, DE, DK, ES, FI, FR, GB, GR, IE, IT, LU, MC, NL, PT, SE).

Published
With international search report.

(54) Title: PROCESS FOR THE MEASUREMENT OF THREE DIMENSIONAL (3D) PROFILES BY MEANS OF STRUCTURED LIGHT PROJECTION

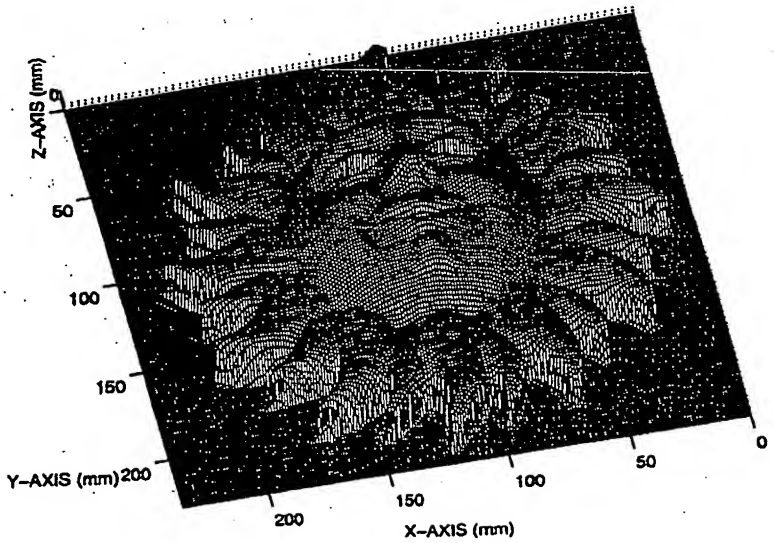

(57) Abstract

Process for the measurement of three dimensional (3D) profiles by means of the projection of structured light, based on the measurement of the shift which each direction of projection undergoes due to the height of the object under measurement. The process includes the steps of determining the shift in pixel of the light codings, and/or of making sinusoidal the projected fringes, and/or of adding an automatic calibration procedure and/or of adding an automatic procedure which determines the geometrical and optical set–up of the system, given as input the required measurement constraints, and/or of integrating the measurement method called GCM with the measurement method called SGM.

FOR THE PURPOSES OF INFORMATION ONLY

Codes used to identify States party to the PCT on the front pages of pamphlets publishing international applications under the PCT.

AL	Albania	ES	Spain	LS	Lesotho	SI	Slovenia
AM	Armenia	FI	Finland	LT	Lithuania	SK	Slovakia
AT	Austria	FR	France	LU	Luxembourg	SN	Senegal
AU	Australia	GA	Gabon	LV	Latvia	SZ	Swaziland
AZ	Azerbaijan	GB	United Kingdom	MC	Monaco	TD	Chad
BA	Bosnia and Herzegovina	GE	Georgia	MD	Republic of Moldova	TG	Togo
BB	Barbados	GH	Ghana	MG	Madagascar	TJ	Tajikistan
BE	Belgium	GN	Guinea	MK	The former Yugoslav Republic of Macedonia	TM	Turkmenistan
BF	Burkina Faso	GR	Greece			TR	Turkey
BG	Bulgaria	HU	Hungary	ML	Mali	TT	Trinidad and Tobago
BJ	Benin	IE	Ireland	MN	Mongolia	UA	Ukraine
BR	Brazil	IL	Israel	MR	Mauritania	UG	Uganda
BY	Belarus	IS	Iceland	MW	Malawi	US	United States of America
CA	Canada	IT	Italy	MX	Mexico	UZ	Uzbekistan
CF	Central African Republic	JP	Japan	NE	Niger	VN	Viet Nam
CG	Congo	KE	Kenya	NL	Netherlands	YU	Yugoslavia
CH	Switzerland	KG	Kyrgyzstan	NO	Norway	ZW	Zimbabwe
CI	Côte d'Ivoire	KP	Democratic People's Republic of Korea	NZ	New Zealand		
CM	Cameroon			PL	Poland		
CN	China	KR	Republic of Korea	PT	Portugal		
CU	Cuba	KZ	Kazakstan	RO	Romania		
CZ	Czech Republic	LC	Saint Lucia	RU	Russian Federation		
DE	Germany	LI	Liechtenstein	SD	Sudan		
DK	Denmark	LK	Sri Lanka	SE	Sweden		
EE	Estonia	LR	Liberia	SG	Singapore		

Title

Process for the measurement of three dimensional (3D) profiles by means of structured light projection.

Description

This invention relates to a process for the measurement of three dimensional (3D) profiles of objects of variable shape by means of the projection of structured light.

As it is well known, the procedure for the measurement of 3D profiles is based on active stereo-vision systems, aimed at measuring the 3D profiles of target objects, and at representing them by means of a point cloud in which each single point represents the X-, Y-, and Z- coordinates of the target object at that point.

It is well known that such a 3D measuring apparatus comprises three basic components, shown in the layout of Figure 1:

the acquisition unit, represented for example by a black and white video-camera, possibly equipped with suitable zoom optics;

the projection unit, represented for example by a projector based on a Liquid Crystal Display (LCD);

the elaboration unit, represented by a Personal Computer for example of the Pentium family, equipped with a suitable frame grabber, on which the measurement procedures are stored.

Figure 1 also shows the optical geometry of such a system. A black and white CCD video camera with 756x581 picture elements acquires the patterns projected by the projection unit, along a different direction with respect to that of projection. Points Ec and Ep, which represent the entrance and exit pupils of the video camera and of the projector respectively, are at a distance L from reference plane R and at a distance d from each other. The optical axes of the video camera and of the projector define a plane which perpendicularly intersects plane R, and

intersect each other at point O on plane R. Parameters FW and FH represent the width of the field of view along the x-coordinate and the y-coordinate respectively. A Personal Computer controls the projector and, through a suitable frame grabber, acquires the images and performs the elaboration. The image resolution is N pixels along the x- coordinate, and M pixels along the y- coordinate. The gray level range is 256.

The 3D profile is obtained by means of triangulation, by observing that the direction of projection described by ray $\overline{EpA}$ is seen by the video camera at point A on plane R when the object is absent, and at point B when the object is present. The height $Z_H(x,y) = \overline{HH'}$ of the object at point H(x,y) can be evaluated by observing that triangles $B\hat{H}A$ and $Ep\hat{H}Ec$ are similar, and that the following triangulation equation holds:

$$Z_H(x,y) = \frac{L \cdot S_R(x,y)}{d + S_R(x,y)} \qquad (1)$$

In Eq.(1) , $S_R(x,y)$ equals segment $\overline{AB}$, and represents the shift that the direction of projection $\overline{EpA}$ undergoes on plane R due to the object height in point H(x,y).

The sensor integrates four measurement methods which differ to each other in the approach used to evaluate shift $S_R(x,y)$. These are:

1. measurement method based on gray code projection (GCM: Gray Code Method);

2. measurement method based on the projection of a single grating (SGM: Single Grating Method);

3. measurement method based on phase shift (PSM: Phase Shift Method);

4. combined method (GCM-PSM: Gray Code Method-Phase Shift Method).

GCM is based on the projection, at *n* successive steps, of *n* different fringe patterns of rectangular profile, to define in the work space 2^n directions of projection, called *light planes*. The stripes are parallel to the *Y*- coordinate. The spatial period of the stripes along the X- direction

varies in such a way that a univocal correspondence is established between the light planes and the words of an n-bit Gray code. Figure 2 schematically shows the resulting attribution of the coding; moreover, it is highlighted that the relation established by the n-bit code words allows the determination of 2^n different directions of projection.

Each pattern is acquired by the video camera and suitable thresholding associates either the logic value '0' or '1' to the gray level of each CCD pixel. This procedure results into a matrix, called *Bit Plane Stack* (BPS), having the same dimensions as the CCD: each element on BPS stores the n-bit Gray code word seen by the corresponding pixel on the CCD. A simple Look-up Table operation allows the conversion of this quantity to the integer light plane number $\hat{i}(j,k)$, where j and k are the discrete coordinates on BPS, and correspond respectively to the X- and Y-coordinates on the reference plane as follows:

$$x = (j - 1/2)\frac{FW}{N} \qquad j=1,...,N \tag{2}$$

$$y = (k - 1/2)\frac{FH}{N} \qquad k=1,....,M \tag{3}$$

The measurement procedure consists of the projection of the same pattern sequence in two different situations, corresponding to the case of absence and presence of the target object on plane R. Two matrices are formed, called BPS_R and BPS_O respectively. Light planes undergo a displacement between BPS_R and BPS_O. Figure 3 gives an idea of (i) how light plane number $\hat{I}(j,k)=0101$ is formed on BPS_R due to the projection on plane R of four patterns (GC_0, GC_1, GC_2, and GC_3, in the figure), and (ii) how it is shifted in BPS_O when an object of parallepipedic shape is supposed to be the target. Shift $S_R(x,y)$ is evaluated by means of the following formula:

$$S_R(x,y) = D_c(j,k)\frac{FW}{N} \tag{4}$$

where parameter $D_c(j,k)$ represents the distance between codings and is obtained by calculating the point by point difference of the light plane codings on BPS_R and BPS_O:

$$D_c(j,k) = K \cdot [BPS\_O(j,k) - BPS\_R(j,k)] \quad (5)$$

where K is a conversion factor from light planes to pixels. Shift $S_R(x,y)$ is then converted into the height by using Eq. (1).

This technique was demonstrated to be particularly appropriate for dealing with steep slope changes and in general shape discontinuities of the surface to be measured, as the evaluation of the height is performed punctually, thus eliminating any influence on the measurement from neighborhood conditions. Moreover, the binarization of the measurement area results into high repeatability of the measurement, and leads to higher values of the measurement precision than those obtained by PSM and SGM.

The methods based on the projection of a single grating (SGM) and on Phase Shift (PSM) associate phase values to light directions, as schematically shown in Figure 4, where it is also highlighted that the same phase value, denoted by θ, is associated to different light directions, making the correspondence non univocal.

Both these method allows the achievement of two phase maps, for the reference and the object respectively, and differ only in the projection sequence and the technique used to perform the phase demodulation.

PSM follows the well-known approach based on the projection of n_p periodic patterns with spatial period p, where each pattern is obtained by spatially shifting the preceding one of a fraction p/n_p of the period. The projected fringes must present a sinusoidal intensity profile. The measurement takes place in two steps: the intensity patterns are firstly projected onto plane R and then the same projection sequence takes place at the target.

Denoting with $I_{Ref,i}(j,k)$ and $I_{Obj,i}(j,k)$ the intensity fields acquired by the video camera in the absence and in the presence of the object

respectively, in correspondence with each shift (i=0, 1, 2, 3), they can be expressed by the two following relationships:

$$I_{Ref,i}(j,k) = a_r(j,k) + \frac{b_r(j,k)}{2}\cos(\omega_x(j + r(j)) - i\frac{\pi}{2}) \quad (6)$$

$$I_{Obj,i}(j,k) = a_o(j,k) + \frac{b_o(j,k)}{2}\cos(\omega_x(j + r(j) + s(j,k)) - i\frac{\pi}{2}) \quad (7)$$

$i=0,1,2,3$

In Eqs.(6) and (7), $a_r(j,k)$ and $a_O(j,k)$ are the average brightness, $b_r(j,k)$ and $b_O(j,k)$ take into account for the fringe contrast for the two cases, ω_X is the spatial frequency of the sinusoidal patterns along the x- direction and r(j) is the lateral shift of the patterns due to the crossed optical axes geometry. Parameter s(j,k) in Eq. (7) is the displacement due to the object. The acquired intensity fields can be combined to get the reference map $\Phi_{Ref}(j,k)$ and the object map $\Phi_{Obj}(j,k)$. These phase maps are evaluated by means of the two following relationships:

$$\Phi_{Ref}(j,k) = \omega_x[j + r(j)] = \text{atan}^{-1}\frac{I_{Ref,1} - I_{Ref,3}}{I_{Ref,0} - I_{Ref,2}} \quad (8)$$

$$\Phi_{Obj}(j,k) = \omega_x[j + r(j) + s(j,k)] = \text{atan}^{-1}\frac{I_{Obj,1} - I_{Obj,3}}{I_{Obj,0} - I_{Obj,2}} \quad (9)$$

Shift $S_R(x,y)$ can be evaluated by means of:

$$S_R(x,y) = \frac{1}{\omega_x}\left[\Phi_{Obj}(j,k) - \Phi_{Ref}(j,k)\right]\cdot\frac{FW}{N} = D_c(j,k)\cdot\frac{FW}{N} \quad (11)$$

where term $\frac{1}{\omega_x}\left[\Phi_{Obj}(j,k) - \Phi_{Ref}(j,k)\right]$ represents distance $D_c(j,k)$ between the phase codings.

In SGM, a single grating of rectangular profile and period *p* is projected both on the reference and on the object to be measured; as schematically shown in Figure 5, it is then demodulated in the time domain by

multiplying each row of the acquired pattern by a sine and a cosine function of the same period; the resulting two signals are then lowpass-filtered and divided by each other. Finally, by evaluating the inverse tangent of this ratio, two phase maps are obtained, respectively called $\Phi_{Ref}(j,k)$ for the reference and $\Phi_{Obj}(j,k)$ for the object, which store, for each element (j,k), the phase value describing the light direction seen by the video camera at the pixel of position (j,k). Shift $S_R(x,y)$ is evaluated by means of Eq. (11).

It is well known that the use of phase values to express directions of projection introduces an ambiguity in the determination of the 3D range information, which is strictly related to the fact that the phase is evaluated mod 2π. Thus, robust unwrapping is needed to evaluate the absolute value of the phase. On the other hand, the phase is continuously distributed on the recorded scene: a good height resolution can be achieved, practically limited only by the errors due to the gray level quantization and to noise.

The experimental work performed shows that good results can be obtained, provided that the object profile is smooth: in this case, the frequency content of the object is in the lower frequency range, and well separated from the grating carrier frequency. However, whenever the maximum phase slope is greater than $2\pi/3p$, being p the grating pitch, the unwrapping of the mod 2π fringe pattern fails, and the absolute phase value cannot be evaluated.

The combination of GCM and PSM is aimed at adding a fractional term to the integer number $\hat{l}(j,k)$ coming from GCM, in order to further decompose each direction of projection. This is obtained by omitting the last pattern from the GCM sequence, by computing the least significant bit (LSB) of the resulting, incomplete coding by means of PSM and by adding a fractional part to the result. As an example, the projection sequence for the case n=4 is shown in Figure 6. The projection sequence is the same as that used in GCM, where the last pattern (GC_3) is omitted, because it is equal to the first pattern of the PSM sequence. The projection of the complete PSM sequence allows the achievement of the phase value. As a

result, real valued light plane number is determined: in the following it is denoted by I(x,y), and expressed by:

$$I(j,k) = \hat{I}(j,k) + \frac{2}{\pi}[\Phi(j,k) + \Delta\Phi(j,k)] \qquad (12)$$

In Eq. (12), term $\hat{I}(j,k)$ represents the incomplete coding, obtained from GCM, with the omission of the last pattern. The phase term $\Phi(j,k)$ is evaluated by means of PSM, without the application of the phase unwrapping algorithm. $\Delta\Phi(j,k)$ represents the phase correction term necessary to achieve the complete encoding, and is evaluated experimentally.

This method allows to further decompose the coding of the light direction from the projector and to code them univocally along the field of view, as schematically shown in Figure 7. The measurement takes place in two steps: the pattern sequence is projected firstly on the reference and then on the object. Two matrices of real values are obtained, called RVLP_R and RVLP_O for the reference and for the object respectively. Shift $S_R(x,y)$ is then calculated by means of the following relation:

$$S_R(x,y) = K \cdot [RVLP\_O(j,k) - RVLP\_R(j,k)] \cdot \frac{FW}{N} = D_c(j,k) \cdot \frac{FW}{N} \qquad (13)$$

where term $K \cdot [RVLP\_O(j,k) - RVLP\_R(j,k)]$ is coding distance $D_c(j,k)$. The height information is then obtained by means of relation (1).

This procedure allows the measurement of objects presenting discontinuities of shapes as well as small details of the surface. In fact, shift $S_R(x,y)$ is obtained by using expression (13), where term Dc(j,k) is a real number instead of an integer, and results into an increased resolution with respect to GCM.

Limitations.

The presented measurement procedure, when performed by using the methods above described, shows a number of drawbacks, in dependence of each single approach.

Limitations of the GCM approach.

Limitation on the width of the measurement area due to the resolution.

The triangulation formula (1) shows that the height resolution depends, among the other parameters, on the minimum value of shift $S_R(x,y)$. In turn, the minimization of $S_R(x,y)$ depends on the reduction of quantities $D_c(j,k)$ and FW in Eq. (4). Dc(j,k) is an integer number, and can not be further reduced. Consequently, the minimization of shift $S_R(x,y)$ can be obtained by reducing value FW, being constant the video camera resolution (N).

Limitation on the width of the measurement area due to the slope error.

The dimension of the measurement area is further reduced by the presence of an error in the measured height which depends on the so called crossed optical axes geometry of the system, where the projection occurs at finite distance from the reference (see Figure 1). Figure 12 shows an example of the measurement of an object of parallepipedic shape (Figure 12.a) and nominal dimensions 137 x 50.4 x 50 (mm). The nominal height is given with uncertainty of 100 μm. Figure 12.b plots the object profile measured along a single section: an error is well observable in the measured height, which presents a slope in correspondence with the top, flat surface of the target. This error is referred to as 'slope error'. It is a systematic error, and directly depends on the fact that in Eq. (4) shift $S_R(x,y)$ is evaluated as a linear function of coding distance $D_c(j,k)$. However, this linear mapping can be successfully applied only if the fringe spatial period p_R can be considered constant on reference R: in fact, in this case, $S_R(x,y)$ linearly depends on difference $D_c(j,k)$ and on period p_R. However, this hypothesis is true only if points Ep and Ec are at infinity; it still holds as far as distance L is sufficiently large and distance d sufficiently small to limit the dependence of p_R on X-. In contrast, for the geometrical setups characterized by reduced values for L and increased values for d, as those typical of GCM, any attempt to evaluate $S_R(x,y)$ by using constant p_R inherently yields an error in the estimation of the height. This error is particular evident when flat surfaces are measured; in fact, the measured profile reveals a slope increasing with both X- and Z-.

Limitation of the measurement area due to the precision of the measurement.

The shift of the codings on matrix BPS_O with respect to their position on BPS_R not only depends on the deformation induced by the object shape, it also depends on the level of uncertainty introduced by the binarization of the gray levels. Since lateral resolution N is a finite value, a number of consecutive elements in the two matrices store the same coding. In the following K_{LP} will be used to indicate this number , with reference to direction of projection LP. The experimental work carried out so far highlighted the dependence of K_{LP} on the threshold value used during the binarization process and the fact that K_{LP} can be different in BPS_O with respect to BPS_R, even for same coding LP. Due to the fact that the comparison between the two matrices is performed by means of a simple difference, it is impossible to isolate and to compensate the contribution on the height errors due to the uncertainty of parameter K_{LP}. This fact results in an increased inaccuracy of the measurement. This effect is well observable in the saw-tooth behavior of the profile shown in Figure 12.b. It increases with K_{LP}, and, for constant N, with increasing values of FW.

Limitations of the approach based on PSM.

Need of a customized projector

The projection sequence of PSM is based on fringe patterns of sinusoidal profile, which can be produced by means of rather sophisticated and expensive projectors.

Limitation on the width of the measurement area due to the slope error.

This limitation is the same as that described for GCM. This is an obvious consequence of the fact that the slope error is due to the crossed optical axes geometry of the system, which is the same for all the methods. Figure 13 shows an example of the slope error in the height evaluated by means of PSM. The same object as in Figure 12.a is measured: obviously the actual height is not revealed by PSM, due to the ambiguity of the phase.

Limitations of the approach SGM.

Limitation on the width of the measurement area due to the slope error.

This limitation is the same as that described for GCM and for PSM. This is an obvious consequence of the fact that the slope error is due to the crossed optical axes geometry of the system, which is the same for all the methods.

Limitations of the combined approach GCM-PSM.

Need of a customized projector.

The projection sequence of GCM-PSM is based on fringe patterns of both rectangular and sinusoidal profile, which can be produced by means of rather sophisticated and expensive projectors.

Limitation on the width of the measurement area due to the slope error.

This limitation is the same as that described for GCM, PSM and SGM. This is an obvious consequence of the fact that the slope error is due to the crossed optical axes geometry of the system, which is the same for all the methods. Figure 14 shows an example of the slope error in the height evaluated by means of GCM-PSM. The same object as in Figure 12.a is measured: the influence of the slope error is the same as that one observed in Figure 12.b, for GCM.

The object of the invention is to develop a process for the measurement of three dimensional profiles of various objects, such that, limitations and drawbacks of the known methods above described can be overcome, and in particular the limitation related to the width of the measurement area due to accuracy and/or precision.

In addition, the object of the invention is to provide a procedure for the measurement of three-dimensional profiles which uses the same device of projection for all the measurement methods and, in particular, avoids the use of sophisticated devices to project fringe patterns of sinusoidal profile.

These and other objects, together with their related advantages described in the following documentation, are obtained by a process for the measurement of three dimensional (3D) profiles by means of the projection of structured light, based on the measurement of the shift ($S_R(x,y)$) that direction of projection EpA undergoes due to the height ($Z_H(x,y)$) of the object under measurement, exploiting the method based on the Gray Code projection (GCM), and/or the method based on the

projection of a single grating (SGM), and/or the method based on the Phase Shift (PSM), and/or the method based on the combination of GCM with PSM (GCM-PSM). This process, in accordance to the invention, includes the following steps:

- the achievement of a reference matrix REF and of an object matrix OBJ and the determination of the shift that the codings of light directions undergo between matrix REF and matrix OBJ, and/or

- the achievement of a sinusoidal profile of the projected fringes, by means of suitable lowpass filtering, and/or

- the introduction of a procedure for the automatic calibration which, starting from a suitable model of the optical geometry of the system, allows the determination of the unknown parameters of such a model by means of an iterative process, and/or

- the introduction of an automatic procedure for the determination of the geometrical and optical set up of the system, on the basis of the required measurement resolution and of the object shape and dimension, and for the determination of the method more suitable to measure the object among the four ones provided, and/or

- the combination of the measurement method based on the projection of Gray Code (GCM) with the measurement method based on the projection of a single grating (SGM).

More in detail, the process as in the invention, includes the following steps:

- projection of the pattern sequence GCM and/or SGM and/or PSM and/or GCM-PSM on the reference;

- achievement of reference matrix REF, where REF coincides with BPS_R in method GCM, with Φ_{Ref} in method PSM and/or SGM, and with RVLP_R in method GCM-PSM;

- projection of the pattern sequence GCM and/or SGM and/or PSM and/or GCM-PSM on the object;

- achievement of object matrix OBJ, where OBJ coincides with BPS_O in method GCM, with Φ_{Obj} in method PSM and/or SGM, and with RVLP_O in method GCM-PSM;

- iterative comparison between the integer part of the elements in matrices REF and OBJ, and determination of the integer part $S_{p,int}(j,k)$ of shift $S_p(j,k)$ by means of the following formula:

$$S_{p.int}(j,k) = j^* - j \tag{10}$$

where j^* and j represent the indexes of the elements that store the same value of the integer part of the coding respectively in matrices OBJ and REF;

- determination of fractional part $S_{p,frac}(j,k)$ of shift $S_p(j,k)$ by means of the following formula:

$$S_{p,frac}(j,k) = \frac{OBJ(j,k) - REF(j,k + S_{p,int}(j,k))}{REF(j,k + S_{p,int}(j,k)) + REF(j,k + S_{p,int}(j,k) - 1)} \tag{40}$$

- determination of shift $S_p(j,k)$ by means of the following formula:

$$S_p(j,k) = S_{p,int}(j,k) + S_{p,frac}(j,k) \tag{41}$$

- conversion of shift $S_p(j,k)$ into shift $S_R(x,y)$ in millimeters by means of the following formula:

$$S_R(x,y) = S_p(j,k) \cdot \frac{FW}{N} \tag{14}$$

- conversion of shift $S_R(x,y)$ into the height by means of Eq. (1).

By means of this process the limitation on the width of the measurement area in methods GCM and/or PSM and/or SGM and/or GCM-PSM is removed: in fact, Eq. (14) represents a simple conversion from shift $S_p(j,k)$, expressed in pixels and shift $S_R(x,y)$, expressed in millimeters; $S_p(j,k)$ is obtained by means of an iterative search of each single coding, which takes into account for that coding LP is stored into K_{LP} consecutive elements in each matrix, and that K_{LP} can be different in the two matrices. Figure 15 shows, for the object in Figure 12.a, the measurement obtained by using the described procedure (bold line) overlapped to that one obtained by using known methods (light line). It is worth noting that the procedure as in the invention results into a strong reduction of the saw-

tooth behavior in the measured profile: this is a direct consequence of the fact that the presence of the same coding into K_{LP} consecutive elements of the coding matrices is accounted for.

Figure 16 plots the profile evaluated in correspondence with the same section as in the previous example when the described procedure is applied to method GCM-PSM (solid line). In the figure, this profile is compared to that obtained by using method GCM-PSM as in the state of the art.

The validity of this procedure is observed even when PSM is used. Figure 17 shows an example. Figure 17.a depicts the target object. The profile measured by using PSM according to the state of the art is shown in Figure 17.b (dashed line), and compared to the profile evaluated when the procedure as in the invention is used in conjunction with PSM (solid line). The measurement errors in correspondence with the maximum height of the object in the two cases are respectively equal to 4.9% and 0.16% of the nominal height. The efficacy of the correction increases with the measuring range along the z coordinate. This behavior is clearly shown in Figure 17.c, where the difference between the two profiles is plotted.

In addition, the process as in the invention of achieving a sinusoidal profile of the projected fringes, includes the following steps:

- projection of the pattern sequence PSM with fringes of rectangular profile on the reference;

- evaluation of the mean spatial period of the fringes, denoted by T, by applying to a single row of one of the acquired intensity pattern the following formula:

$$T = \left[\frac{FW}{\max} + \frac{FW}{\min}\right] \Big/ 2 \qquad (18)$$

where max and min represent respectively the number of maxima and of minima detected on the row by using an algorithm for the evaluation of positive and negative peaks;

- evaluation of the cut-off frequency of the lowpass filter by means of the following formula:

$$f_t = \frac{3}{2T} \tag{17}$$

- elaboration of terms $\Delta I_{Ref,Num}$ and $\Delta I_{Ref,Den}$ by means of the lowpass filter and evaluation of the ratio between the two resulting signals;

- determination of reference matrix $\Phi_{Ref}(j,k)$ by means of known Eq. (8);

- projection of the pattern sequence PSM with fringes of rectangular profile on the object;

- elaboration of terms $\Delta I_{Obj,Num}$ and $\Delta I_{Obj,Den}$ by means of the lowpass filter and evaluation of the ratio between the two resulting signals;

- determination of object matrix $\Phi_{Obj}(j,k)$ by means of known Eq. (9);

- evaluation of shift $S_R(x,y)$ by means of known relation (11) or (14);

- evaluation of the height by means of known Eq. (1).

By using this process a lowpass filtering operation is applied to the components at the numerator and at the denominator of each one of the following expressions:

$$\frac{\Delta I_{Ref,Num}}{\Delta I_{Ref,Den}} = \frac{I_{Ref,1} - I_{Ref,3}}{I_{Ref,0} - I_{Ref,2}} = \frac{\sum_{n=0}^{\infty} B_{Ref,n}(j,k) \cdot \sin[n \cdot \omega_x (j + r(j))]}{\sum_{n=0}^{\infty} B_{Ref,n}(j,k) \cdot \cos[n \cdot \omega_x (j + r(j))]} \tag{15}$$

$$\frac{\Delta I_{Obj,Num}}{\Delta I_{Obj,Den}} = \frac{I_{Obj,1} - I_{Obj,3}}{I_{Obj,0} - I_{Obj,2}} = \frac{\sum_{n=0}^{\infty} B_{Obj,n}(j,k) \cdot \sin[n \cdot \omega_x (j + r(j) + s(j,k))]}{\sum_{n=0}^{\infty} B_{Obj,n}(j,k) \cdot \cos[n \cdot \omega_x (j + r(j) + s(j,k))]} \tag{16}$$

In Eqs. (15) and (16) terms $I_{Ref,i}(j,k)$ and $I_{Obj,i}(j,k)$ refer to the intensity fields acquired by the video camera in the absence and in the presence of the object respectively, in correspondence with each shift (i=0,1,2,3), and the presence of an infinite number of spectral components is evidenced, due to the rectangular intensity profile of the fringes. The difference operation which determines terms $\Delta I_{Ref,Num}$, $\Delta I_{Ref,Den}$, $\Delta I_{Obj,Num}$, $\Delta I_{Obj,Den}$, eliminates the even spectral components while leaves all the odd components. Thus, the filtering operation is aimed at eliminating all the odd spectral components with the exception of that one at the fundamental frequency: this situation is the same as if the projected fringes had sinusoidal profile.

This procedure utilizes a Butterworth lowpass filter of the fourth order, implemented as an IIR filter, using the well known bilinear transformation technique and compensating for the filter phase non linearity by filtering the signal forward and backward. The filter cut-off frequency is adaptive, since it is expressed as a function of mean spatial period T of the projected fringes, represented by Eq. (17).

By means of this process the limitation on the need of a device specialized to the projection of sinusoidal fringes is removed; instead it is possible to use the device utilized to project the pattern sequences of GCM, SGM, which are all based on fringes of rectangular profile, even for the projection of both PSM and GCM-PSM pattern sequences.

Figure 18.a shows the 3D profile reconstruction of an object obtained by using method GCM-PSM without using the filtering process. This profile should be compared with that one obtained by means of the novel filtering process, shown in Figure 18.b. The former profile (Figure 18.a) is characterized by a precision of 150 μm, whilst the latter (Figure 18.b) shows a precision of 40 μm.

In addition, the process as in the invention, of introducing a procedure for the automatic calibration of the system, is based on the following steps:

- projection of the pattern sequence GCM and/or SGM and/or PSM and/or GCM-PSM on the reference and on the object;

- evaluation of light planes on the reference and on the object;

- setting of the height tolerance Δm;

- evaluation of initial values α_0 of angle α, defined by the intersection between the projection plane within the projector and the reference plane, and of initial value γ_0 of angle γ, defined by the intersection between the first ray seen by the video camera and the perpendicular line to the reference plane, by using the following formulas:

$$\alpha_0 = \text{atan}\left(\frac{d_0}{L_0}\right) \qquad (22)$$

$$\gamma_0 = \operatorname{atan}\left(\frac{d_0 - \frac{FW}{2}}{L_0}\right) \qquad (23)$$

- reconstruction of the profile of the calibration object by using estimates α_0 and γ_0;

- determination of those pixels which image the object;

- evaluation of the linear regression of the calculated heights;

- evaluation of $\alpha_{i+1} = (1 + p_{\alpha i} \cdot m_i) \cdot \alpha_i$ with term $p_{\alpha i} > 0$;

- reconstruction of the profile of the calibration object by using current estimates of α and γ;

- evaluation of the linear regression of the calculated heights;

- if the module of the resulting angular coefficient is greater than that one at the previous step, the sign of term $p_{\alpha i}$ is inverted;

- resetting of the initial conditions and execution of the same sequence of steps for the determination of angle γ; if it is necessary, the sign of term $p_{\gamma i}$ is inverted;

- optimization cycle:

  while coefficient m_i is greater than the preset tolerance Δm, new values for angles α and γ are derived by means of the following formulas:

$$\alpha_{i+1} = (1 + p_{\alpha i} \cdot m_i) \cdot \alpha_i \qquad (24)$$

$$\gamma_{i+1} = (1 + p_{\gamma i} \cdot m_i) \cdot \gamma_i \qquad (25)$$

- the linear regression on the measured profile is performed, angular coefficient m_{i+1} is evaluated, and the cycle convergence is checked; if the cycle diverges those values for angles α and γ evaluated at previous iteration are assigned to current values, and parameters $p_{\alpha i}$ and $p_{\gamma i}$ are decremented.

This process allows the transformation of phase matrices $\Phi_{Obj}(j,k)$ and $\Phi_{Ref}(j,k)$ in Eq.(11) and of real valued matrices RVLP_O(j,k) and RVLP_R(j,k) in Eq. (13) into abscissas matrices, according to the model of

the system optical geometry presented in Figure 8, by using the following expressions:

$$X_O(j,k) = L \cdot \left(\tan\left(\gamma - \operatorname{atan}\left(\frac{\frac{OBJ(j,k) \cdot \sin(\delta_{tot})}{nlp \cdot \sin(\theta_{tot})} \cdot \cos(\gamma - \alpha)}{1 + \frac{OBJ(j,k) \cdot \sin(\delta_{tot})}{nlp \cdot \sin(\theta_{tot})} \cdot \sin(\gamma - \alpha)} \right) \right) \right) \quad (19)$$

$$X_R(j,k) = L \cdot \left(\tan\left(\gamma - \operatorname{atan}\left(\frac{\frac{REF(j,k) \cdot \sin(\delta_{tot})}{nlp \cdot \sin(\theta_{tot})} \cdot \cos(\gamma - \alpha)}{1 + \frac{REF(j,k) \cdot \sin(\delta_{tot})}{nlp \cdot \sin(\theta_{tot})} \cdot \sin(\gamma - \alpha)} \right) \right) \right) \quad (20)$$

where REF(j,k) and OBJ(j,k) are the codings of the light planes, and thus correspond to elements BPS_R(j,k) and BPR_O(j,k) and/or to elements $\Phi_{Ref}(j,k)$ and $\Phi_{Obj}(j,k)$ and/or to elements RVLP_R(j,k) and RVLP_O(j,k). Eqs.(19) and (20) are applied after the determination of the matrices storing the light plane codings. The whole elaboration scheme is shown in Figure 9.

This process as in the invention increases the accuracy in the evaluation of the height, since shift $S_R(x,y)$ is determined by means of the following formula:

$$[X_O(j,k) - X_R(j,k)] \quad (21)$$

which represents a simple difference between abscissa values.

The use of Eqs. (19) and (20) is possible only if two new angles are known, called α and γ. These are shown in Figure 8, and represent respectively the angle defined by the intersection between the projection plane within the projector and the reference plane, and the angle between the first light direction seen by the video camera (ray E_pS in the figure) and the perpendicular line E_pR to the reference plane. These angles are unknown and must be determined by means of a suitable calibration procedure.

This procedure is iterative and automatically determines angles α and γ. It is based on the minimization of a suitable parameter, correlated with the effect of the slope error on the measured height. This parameter is

denoted in the following by m, and represents the angular coefficient of the linear regression evaluated on the height measured on a calibration master of parallepipedic shape. Before the calibration of the profilometer, the system geometry is not precisely known, and the initial values for angles α and γ are defined by considering the simplified geometry in Figure 10. The orientation of the projection plane is unknown: for simplicity it is initially assumed that it is perpendicular to the projector optical axis, with an uncertainty of ±15°. Thus, the initial estimate on angle α is determined by:

$$\alpha_0 = \text{atan}\left(\frac{d_0}{L_0}\right) \tag{22}$$

where L_0 and d_0 are initial estimates of parameters L and d.

Initial value γ_0 of angle γ is evaluated by considering triangle EpŜQ as:

$$\gamma_0 = \text{atan}\left(\frac{d_0 - \frac{FW}{2}}{L_0}\right) \tag{23}$$

From this initial condition the calibration process evolves exploiting the information related to the angular coefficient m of the linear regression evaluated over the profile measured along a single section of the calibration master. Angles α and γ are evaluated by means of Eqs. (24) and (25) in order to reduce step by step angular coefficient m.

Values α_{i+1} and γ_{i+1} are determined from current values α_i and γ_i, by multiplying them respectively by factor $(1 + p_{\alpha i} \cdot m_i)$ and factor $(1 + p_{\gamma i} \cdot m_i)$, where $p_{\alpha i}$ and $p_{\gamma i}$ are weights, experimentally determined. At each iteration, by using the new values for α and γ the master profile is evaluated along the section, and the corresponding angular coefficient m is determined. This iteration stops when coefficient m is within tolerance Δm.

The significance of such formulas (24) and (25) is clear: the higher the value of m, the higher the variation induced on values α_{i+1} and γ_{i+1}; if, on the contrary, angular coefficient m is small, only small variations will be

produced from α_i and γ_i, to α_{i+1} and γ_{i+1}, which are actually close to the search solution.

By means of this procedure, the measurement area can be increased, since shift $S_R(x,y)$ is evaluated directly as the difference between abscissa values on the reference, as expressed by Eq. (21), instead of using difference $D_c(j,k)$ between codings of light planes. Figure 19 shows the height profile in correspondence with a single section of the object in Figure 12.a, measured by using such a calibration process in combination with GCM (solid line). In the figure, this profile is compared to that one resulting from the utilization of GCM without the proposed calibration (dashed line). The measurement error is reduced from 25.3% to 0.08% of the nominal height of the object. Figures 20 and Figure 21 show the effect of the introduction of such a calibration process in conjunction with method GCM-PSM (Figure 20) and method PSM (Figure 21). Both the figures plot the profiles measured by using the calibration process (solid line) and by conventional GCM-PSM and PSM (dashed line). In both the experiments a strong reduction of the measurement error can be observed, of the same entity as that evaluated in correspondence with GCM.

In addition, the process as in the invention, of introducing an automatic procedure for the determination of the geometrical and optical set up of the system, and of the method more suitable to measure the object among the four ones provided, including the following steps:

- input statement of the object dimensions denoted by X, Y, and Z;
- input statement of the required measurement resolution z_{min};
- input statement of the shape characteristics of the object;
- evaluation of the field of view FW by means of the following relation:

$$FW = 1.7 \cdot \max(X, Y) \tag{26}$$

- evaluation of parameter L by means of the following formula:

$$L = 10 \cdot Z \tag{27}$$

- evaluation of focal length of the video-camera by using the following formula:

$$f = k_1 \cdot L / FW \quad (28)$$

where k1 is experimentally determined;

- evaluation of focal number f# by means of:

$$f\# = k_2 \cdot Z \cdot f^2 / L^2 \quad (29)$$

where k_2 is experimentally determined;

- choice of the measurement method among GCM, PSM, SGM and GCM-PSM, in dependence on both the topology of the object and required z_{min};

- evaluation of the value of parameter d by using the following formulas:

$$d = \frac{FW \cdot L}{N \cdot z_{min}} \quad (30)$$

$$d = \frac{L \cdot p \cdot \Phi_{min} - p \cdot \Phi_{min} \cdot z_{min}}{2 \cdot p \cdot z_{min}} \quad (31)$$

where p represents the spatial period of the projected fringe pattern presenting minimum period among those patterns of the chosen projection sequence, and Φ_{min} is the minimum phase value achievable, depending on the acquisition device; Eq. (30) is used when GCM is selected to perform the measurement, while Eq. (31) is used in conjunction with the other methods;

- output of the optical and geometrical parameters determined (f, f#, FW, L, d), and of the suggested projection method.

Such a procedure makes the set-up phase of the system completely automatic, and considerably simplifies the use of the system, even for non skilled users. In fact, the evaluation of the critical parameters is performed by the process itself, which determines the best values for :

- field of view FW;

- distance of the projector from the video-camera (d);

- stand-off distance L;

- focal length f;

- the most suitable projection method among those available (GCM, PSM, SGM and GCM-PSM),

in order to guarantee the required resolution. The structure of the process is schematically shown in Figure 11.

In addition, the process as in the invention, of introducing a procedure for the combination of the measurement method based on the projection of Gray Code (GCM) with the measurement method based on the projection of a single grating (SGM), is based on the following steps:

- projection of (n-1) patterns of the pattern sequence of GCM on the reference;

- evaluation of the incomplete coding of light planes $\hat{I}_{Ref}(j,k)$;

- projection of the n-th pattern on the reference;

- evaluation of phase $\Phi_{Ref}(j,k)$ on the reference by using method SGM;

- evaluation of matrix REF of real valued light planes on the reference. Denoting with $I_{Ref}(j,k)$ the element stored into the matrix at position (j,k), it is evaluated by using the following formula:

$$I_{Ref}(j,k) = \hat{I}_{Ref}(j,k) + \frac{2}{\pi}\left[\Phi_{Ref}(j,k) + \Delta\Phi(j,k)\right] \qquad (33)$$

where $\Delta\Phi(j,k)$ represents the correction term needed to eliminate the incompleteness of GCM;

- projection of (n-1) patterns of the pattern sequence of GCM on the object;

- evaluation of the incomplete coding of light planes $\hat{I}_{Obj}(j,k)$;

- projection of the n-th pattern on the object;

- evaluation of phase $\Phi_{Obj}(j,k)$ on the object by using method SGM;

- evaluation of matrix OBJ of real valued light planes on the object. Denoting with $I_{Obj}(j,k)$ the element stored into the matrix at position (j,k), it is evaluated by using the following formula:

$$I_{Obj}(j,k) = \hat{I}_{Obj}(j,k) + \frac{2}{\pi}\left[\Phi_{Obj}(j,k) + \Delta\Phi(j,k)\right] \qquad (34)$$

where $\Delta\Phi(j,k)$ represents the correction term needed to eliminate the incompleteness of GCM;

- conversion of matrices REF and OBJ by means of Eq. (19) and (20);
- evaluation of shift $S_R(x,y)$ by means of Eq.(21);
- evaluation of the height by means of Eq.(1).

Such a procedure allows the reconstruction of the 3D profiles of objects presenting steep slope changes as well as fine details as in method GCM-PSM, while reducing the number of the projection patterns from (n+np+1), as in GCM-PSM to value n. The procedure combines method GCM with method SGM, in such a way that two matrices REF and OBJ are obtained, for the reference and for the object respectively, storing real valued elements I(j,k), expressed by:

$$I(j,k) = \hat{I}(j,k) + \frac{2}{\pi}[\Phi(j,k) + \Delta\Phi(j,k)] \qquad (35)$$

In Eq. (35), term $\hat{I}(j,k)$ represents the contribution to the coding determined by GCM, whilst $\Phi(j,k)$ is the phase term evaluated by SGM.

This procedure allows to further decompose the light directions from the projector with respect to the integer coding achievable by using GCM, and, at the same time, to univocally determine each direction of projection along the whole field of view FW.

The procedure as in the invention of automatic calibration can be then exploited, to determine angles α and γ, and then the light plane codings can be converted into abscissa values by using Eqs. (19) and (20). The use of Eq.(21) to determine shift $S_R(x,y)$ avoids the influence of the slope error on the measured height.

The invention is illustrated with reference to the following drawings, given to exemplify and not to limit the invention itself, wherein:

Figure 1 shows the commonly used layout of the system, together with its optical geometry;

Figure 2 highlights the coding of light planes performed by means of GCM;

Figure 3 shows an example of the GCM projection sequence of 4 patterns on the reference plane (i) and in the presence of the measured object (ii);

Figure 4 shows the phase coding attribution to each direction of projection by using methods PSM or SGM: same phase value θ is given to more than one light ray;

Figure 5 schematically shows the SGM procedure

Figure 6 shows an example of the projection sequence in the combined procedure GCM-PSM, for n equal to 4;

Figure 7 highlights the coding of real valued light planes obtained by combining GCM to PSM;

Figure 8 shows the advanced model of the optical geometry;

Figure 9 data elaboration flow chart after the introduction of the novel projective model;

Figure 10 geometric model used to determine the initial conditions on angles α and γ;

Figure 11 shows the flow chart of the optical CAD automatic procedure;

Figure 12.a and 12.b respectively show a target chosen for the measurement and the profile along a single section measured by using conventional methods;

Figure 13 shows the influence of the slope error when the method based on PSM is used;

Figure 14 shows an example of the influence of the slope error when the method based on GCM-PSM is exploited;

Figure 15 shows the correction of the slope error in the method based on GCM by using the search-based procedure;

Figure 16 shows the correction of the slope error in the method based on GCM-PSM by using the search-based procedure;

Figures 17.a, 17.b, 17.c show the correction of the slope error in the method based on PSM by using the search-based procedure;

Figure 18 shows the effect of the filtering procedure used in PSM: 18.a: measurement performed without the filtering operation; 18.b: measurement performed with the filtering procedure;

Figure 19 shows the correction of the slope error in method GCM by means of the procedure for calibrating angles α and γ;

Figure 20 shows the correction of the slope error in method GCM-PSM by means of the procedure for calibrating angles α and γ;

Figure 21 shows the correction of the slope error in method PSM by means of the procedure for calibrating angles α and γ;

Claims

1. process for the measurement of three dimensional (3D) profiles by means of the projection of structured light, based on the measurement of the shift ($S_R(x,y)$) that direction of projection EpA undergoes due to the height ($Z_H(x,y)$) of the object under measurement, exploiting the method based on the Gray Code projection (GCM), and/or the method based on the projection of a single grating (SGM), and/or the method based on the Phase Shift (PSM), and/or the method based on the combination of GCM with PSM (GCM-PSM). This process, in accordance to the invention, includes the following steps:

- the achievement of a reference matrix REF and of an object matrix OBJ and the determination of the shift that the codings of light directions undergo between matrix REF and matrix OBJ, and/or

- the achievement of a sinusoidal profile of the projected fringes, by means of suitable lowpass filtering, and/or

- the introduction of a procedure for the automatic calibration which, starting from a suitable model of the optical geometry of the system, allows the determination of the unknown parameters of such a model by means of an iterative process, and/or

- the introduction of an automatic procedure for the determination of the geometrical and optical set up of the system, on the basis of the required measurement resolution and of the object shape and dimension, and for the determination of the method more suitable to measure the object among the four ones provided, and/or

- the combination of the measurement method based on the projection of Gray Code (GCM) with the measurement method based on the projection of a single grating (SGM).

2. A process, according to claim 1, characterized in that it includes the following steps:

- projection of the pattern sequence GCM and/or SGM and/or PSM and/or GCM-PSM on the reference;

- achievement of reference matrix REF, where REF coincides with BPS_R in method GCM, with Φ_{Ref} in method PSM and/or SGM, and with RVLP_R in method GCM-PSM;

- projection of the pattern sequence GCM and/or SGM and/or PSM and/or GCM-PSM on the object;

- achievement of object matrix OBJ, where OBJ coincides with BPS_O in method GCM, with Φ_{Obj} in method PSM and/or SGM, and with RVLP_O in method GCM-PSM;

- iterative comparison between the integer part of the elements in matrices REF and OBJ, and determination of the integer part $S_{p,int}(j,k)$ of shift $S_p(j,k)$ by means of the following formula:

$$S_{p,int}(j,k) = j^* - j \qquad (10)$$

where j^* and j represent the indexes of the elements that store the same value of the integer part of the coding respectively in matrices OBJ and REF;

- determination of fractional part $S_{p,frac}(j,k)$ of shift $S_p(j,k)$ by means of the following formula:

$$S_{p,frac}(j,k) = \frac{OBJ(j,k) - REF(j,k + S_{p,int}(j,k))}{REF(j,k + S_{p,int}(j,k)) + REF(j,k + S_{p,int}(j,k) - 1)} \qquad (40)$$

- determination of shift $S_p(j,k)$ by means of the following formula:

$$S_p(j,k) = S_{p,int}(j,k) + S_{p,frac}(j,k) \qquad (41)$$

- conversion of shift $S_p(j,k)$ into shift $S_R(x,y)$ in millimeters by means of the following formula:

$$S_R(x,y) = S_p(j,k) \cdot \frac{FW}{N} \qquad (14)$$

- conversion of shift $S_R(x,y)$ into the height by means of Eq. (1).

3. A process according to claim 1, characterized in that it achieves a sinusoidal profile of the projected fringes, including the following steps:

- projection of the pattern sequence PSM with fringes of rectangular profile on the reference;

- evaluation of the mean spatial period of the fringes, denoted by T, by applying to a single row of one of the acquired intensity pattern the following formula:

$$T = \left[\frac{FW}{\max} + \frac{FW}{\min}\right] \Big/ 2 \qquad (18)$$

where max and min represent respectively the number of maxima and of minima detected on the row by using an algorithm for the evaluation of positive and negative peaks;

- evaluation of the cut-off frequency of the lowpass filter by means of the following formula:

$$f_t = \frac{3}{2T} \qquad (17)$$

- elaboration of terms $\Delta I_{Ref,Num}$ and $\Delta I_{Ref,Den}$ by means of the lowpass filter and evaluation of the ratio between the two resulting signals;

- determination of reference matrix $\Phi_{Ref}(j,k)$ by means of known Eq. (8);

- projection of the pattern sequence PSM with fringes of rectangular profile on the object;

- elaboration of terms $\Delta I_{Obj,Num}$ and $\Delta I_{Obj,Den}$ by means of the lowpass filter and evaluation of the ratio between the two resulting signals;

- determination of object matrix $\Phi_{Obj}(j,k)$ by means of known Eq. (9);

- evaluation of shift $S_R(x,y)$ by means of known relation (11) or (14);

- evaluation of the height by means of known Eq. (1).

4. A process according to claim 3, characterized in that it utilizes a Butterworth lowpass filter of the fourth order, implemented as an IIR filter, with adaptive cut-off frequency.

5. A process according to claim 1, characterized in that it introduces the automatic calibration of the system, based on the following steps:

- projection of the pattern sequence GCM and/or SGM and/or PSM and/or GCM-PSM on the reference and on the object;

- evaluation of light planes on the reference and on the object;

- setting of the height tolerance Δm;

- evaluation of initial values α_0 of angle α, defined by the intersection between the projection plane within the projector and the reference plane, and of initial value γ_0 of angle γ, defined by the intersection between the first ray seen by the video camera and the perpendicular line to the reference plane, by using the following formulas:

$$\alpha_0 = \text{atan}\left(\frac{d_0}{L_0}\right) \tag{22}$$

$$\gamma_0 = \text{atan}\left(\frac{d_0 - \frac{FW}{2}}{L_0}\right) \tag{23}$$

- reconstruction of the profile of the calibration object by using estimates α_0 and γ_0;

- determination of those pixels which image the object;

- evaluation of the linear regression of the calculated heights;

- evaluation of $\alpha_{i+1} = (1 + p_{\alpha i} \cdot m_i) \cdot \alpha_i$ with term $p_{\alpha i} > 0$;

- reconstruction of the profile of the calibration object by using current estimates of α and γ;

- evaluation of the linear regression of the calculated heights;

- if the module of the resulting angular coefficient is greater than that one at the previous step, the sign of term $p_{\alpha i}$ is inverted;

- resetting of the initial conditions and execution of the same sequence of steps for the determination of angle γ; if it is necessary, the sign of term $p_{\gamma i}$ is inverted;

- optimization cycle:

  while coefficient m_i is greater than the preset tolerance Δm, new values for angles α and γ are derived by means of the following formulas:

$$\alpha_{i+1} = (1 + p_{\alpha i} \cdot m_i) \cdot \alpha_i \tag{24}$$

$$\gamma_{i+1} = (1 + p_{\gamma i} \cdot m_i) \cdot \gamma_i \tag{25}$$

- the linear regression on the measured profile is performed, angular coefficient m_{i+1} is evaluated, and the cycle convergence is checked; if the

cycle diverges those values for angles α and γ evaluated at previous iteration are assigned to current values, and parameters $p_{\alpha i}$ and $p_{\gamma i}$ are decremented.

6. A process according to claim 5, characterized in that phase matrices $\Phi_{Obj}(j,k)$ and $\Phi_{Ref}(j,k)$ in Eq.(11) and of real valued matrices RVLP_O(j,k) and RVLP_R(j,k) in Eq. (13) into abscissas matrices, according to the model of the system optical geometry presented in Figure 8, by using the following expressions:

$$X_o(j,k) = L \cdot \left(\tan\left(\gamma - \operatorname{atan}\left(\frac{\frac{OBJ(j,k)\cdot \sin(\delta_{tot})}{nlp \cdot \sin(\theta_{tot})} \cdot \cos(\gamma - \alpha)}{1 + \frac{OBJ(j,k)\cdot \sin(\delta_{tot})}{nlp \cdot \sin(\theta_{tot})} \cdot \sin(\gamma - \alpha)} \right) \right) \right) \quad (19)$$

$$X_R(j,k) = L \cdot \left(\tan\left(\gamma - \operatorname{atan}\left(\frac{\frac{REF(j,k)\cdot \sin(\delta_{tot})}{nlp \cdot \sin(\theta_{tot})} \cdot \cos(\gamma - \alpha)}{1 + \frac{REF(j,k)\cdot \sin(\delta_{tot})}{nlp \cdot \sin(\theta_{tot})} \cdot \sin(\gamma - \alpha)} \right) \right) \right) \quad (20)$$

where REF(j,k) and OBJ(j,k) are the codings of the light planes, and thus correspond to elements BPS_R(j,k) and BPR_O(j,k) and/or to elements $\Phi_{Ref}(j,k)$ and $\Phi_{Obj}(j,k)$ and/or to elements RVLP_R(j,k) and RVLP_O(j,k). Eqs.(19) and (20) are applied after the determination of the matrices storing the light plane codings.

7. A process according to claims 5 and 6, characterized in that shift $S_R(x,y)$ is determined by means of the following formula:

$$[X_O(j,k) - X_R(j,k)] \quad (21)$$

8. A process according to claim 1, characterized by an automatic procedure for the determination of the geometrical and optical set up of the system, and of the method more suitable to measure the object among the four ones provided, including the following steps:

- input statement of the object dimensions denoted by X, Y, and Z;
- input statement of the required measurement resolution z_{min};
- input statement of the shape characteristics of the object;

- evaluation of the field of view FW by means of the following relation:

$$FW = 1.7 \cdot \max(X, Y) \tag{26}$$

- evaluation of parameter L by means of the following formula:

$$L = 10 \cdot Z \tag{27}$$

- evaluation of focal length of the video-camera by using the following formula:

$$f = k_1 \cdot L / FW \tag{28}$$

where k1 is experimentally determined;

- evaluation of focal number f# by means of:

$$f\# = k_2 \cdot Z \cdot f^2 / L^2 \tag{29}$$

where k_2 is experimentally determined;

- choice of the measurement method among GCM, PSM, SGM and GCM-PSM, in dependence on both the topology of the object and required z_{min};

- evaluation of the value of parameter d by using the following formulas:

$$d = \frac{FW \cdot L}{N \cdot z_{min}} \tag{30}$$

$$d = \frac{L \cdot p \cdot \Phi_{min} - p \cdot \Phi_{min} \cdot z_{min}}{2 \cdot p \cdot z_{min}} \tag{31}$$

where p represents the spatial period of the projected fringe pattern presenting minimum period among those patterns of the chosen projection sequence, and Φ_{min} is the minimum phase value achievable, depending on the acquisition device; Eq. (30) is used when GCM is selected to perform the measurement, while Eq. (31) is used in conjunction with the other methods;

- output of the optical and geometrical parameters determined (f, f#, FW, L, d), and of the suggested projection method.

9. A process according to claim 1, characterized in that it introduces a procedure for the combination of the measurement method based on the projection of Gray Code (GCM) with the measurement method based on the projection of a single grating (SGM), based on the following steps:

- projection of (n-1) patterns of the pattern sequence of GCM on the reference;

- evaluation of the incomplete coding of light planes $\hat{I}_{Ref}(j,k)$;

- projection of the n-th pattern on the reference;

- evaluation of phase $\Phi_{Ref}(j,k)$ on the reference by using method SGM;

- evaluation of matrix REF of real valued light planes on the reference. Denoting with $I_{Ref}(j,k)$ the element stored into the matrix at position (j,k), it is evaluated by using the following formula:

$$I_{Ref}(j,k) = \hat{I}_{Ref}(j,k) + \frac{2}{\pi}\left[\Phi_{Ref}(j,k) + \Delta\Phi(j,k)\right] \qquad (33)$$

where $\Delta\Phi(j,k)$ represents the correction term needed to eliminate the incompleteness of GCM;

- projection of (n-1) patterns of the pattern sequence of GCM on the object;

- evaluation of the incomplete coding of light planes $\hat{I}_{Obj}(j,k)$;

- projection of the n-th pattern on the object;

- evaluation of phase $\Phi_{Obj}(j,k)$ on the object by using method SGM;

- evaluation of matrix OBJ of real valued light planes on the object. Denoting with $I_{Obj}(j,k)$ the element stored into the matrix at position (j,k), it is evaluated by using the following formula:

$$I_{Obj}(j,k) = \hat{I}_{Obj}(j,k) + \frac{2}{\pi}\left[\Phi_{Obj}(j,k) + \Delta\Phi(j,k)\right] \qquad (34)$$

where $\Delta\Phi(j,k)$ represents the correction term needed to eliminate the incompleteness of GCM;

- conversion of matrices REF and OBJ by means of Eq. (19) and (20);

- evaluation of shift $S_R(x,y)$ by means of Eq.(21);

- evaluation of the height by means of Eq.(1).

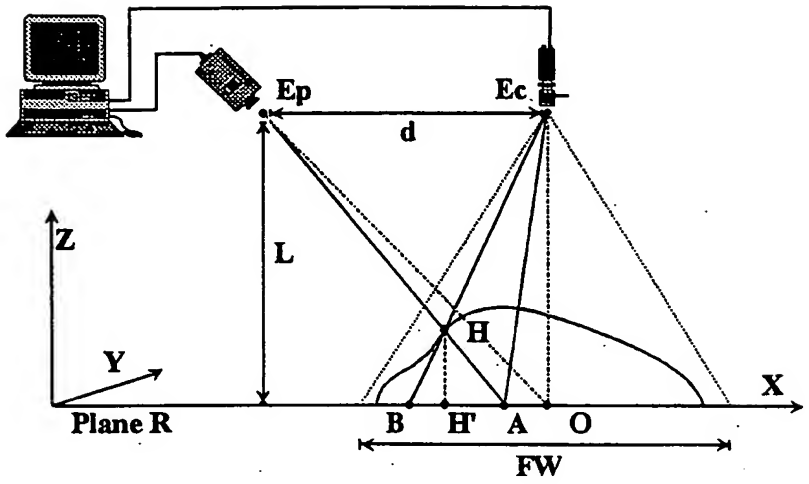
Ep
Ec
d
Z
L
Y
H
X
Plane R
B
H'
A
O
FW

Fig. 1

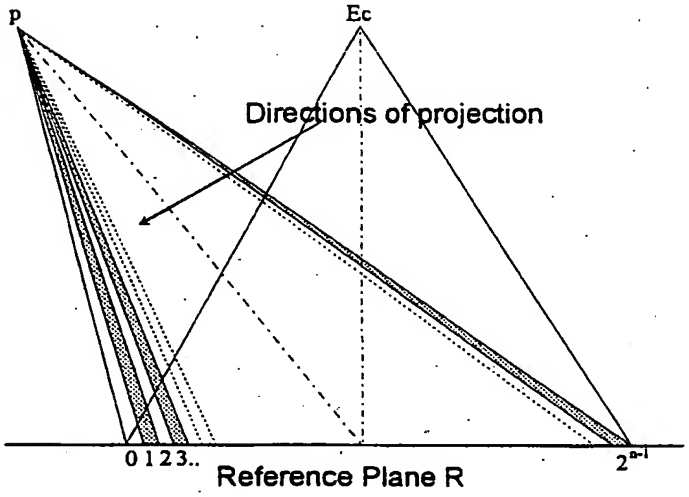
p
Ec
Directions of projection
0 1 2 3..
Reference Plane R
2^n-1

Fig. 2.

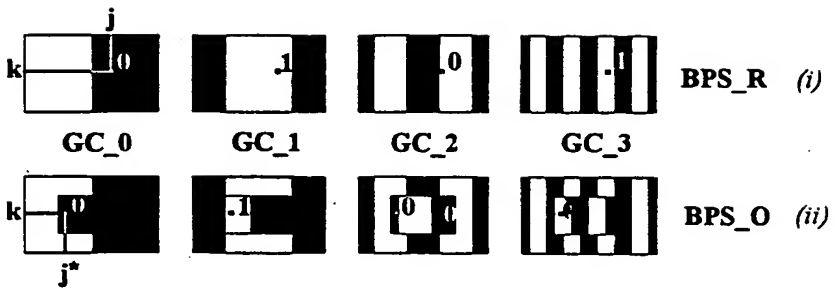
j
k
0
1
0
1
BPS_R (i)
GC_0
GC_1
GC_2
GC_3
k
0
1
0
BPS_O (ii)
j*

Fig . 3.

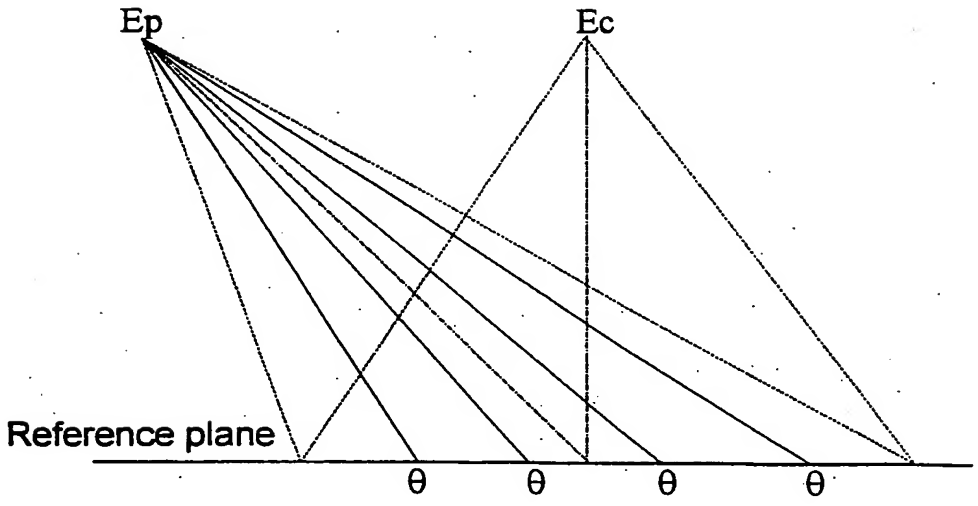
Ep
Ec
Reference plane
θ
θ
θ
θ

Fig . 4.

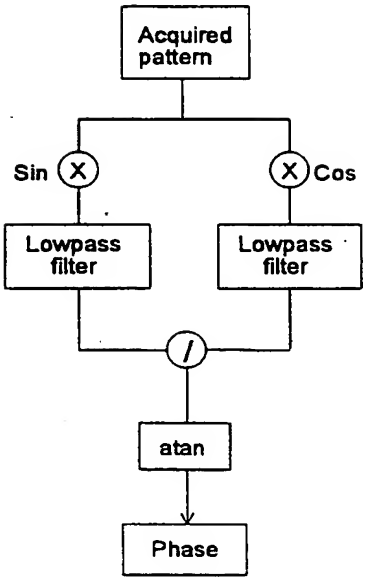

Figure 5.

Fig. 6.

4/16

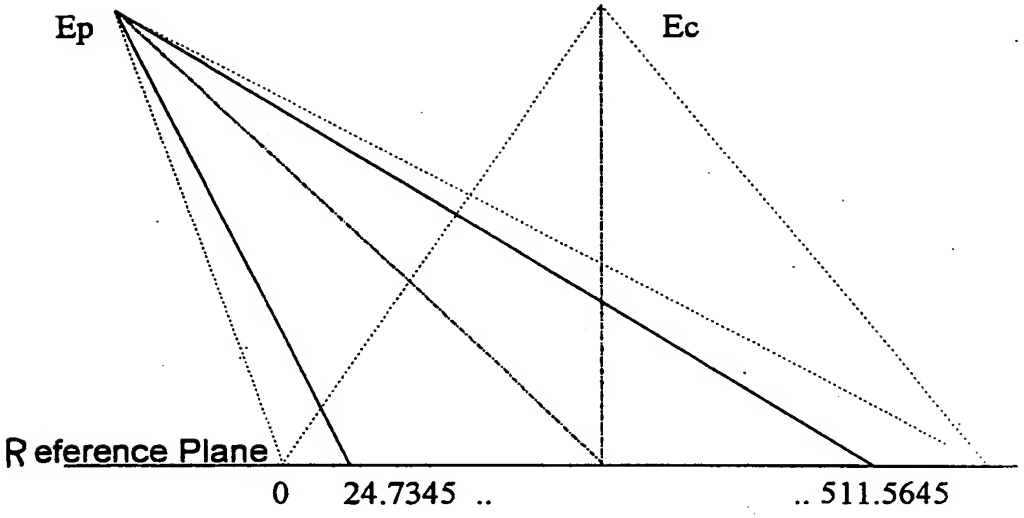

Fig . 7

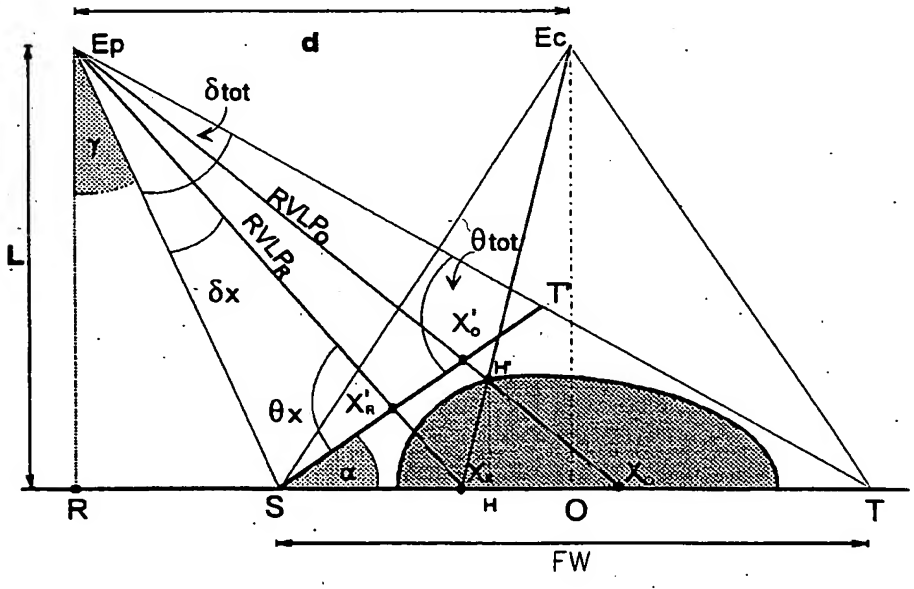

Fig . 8

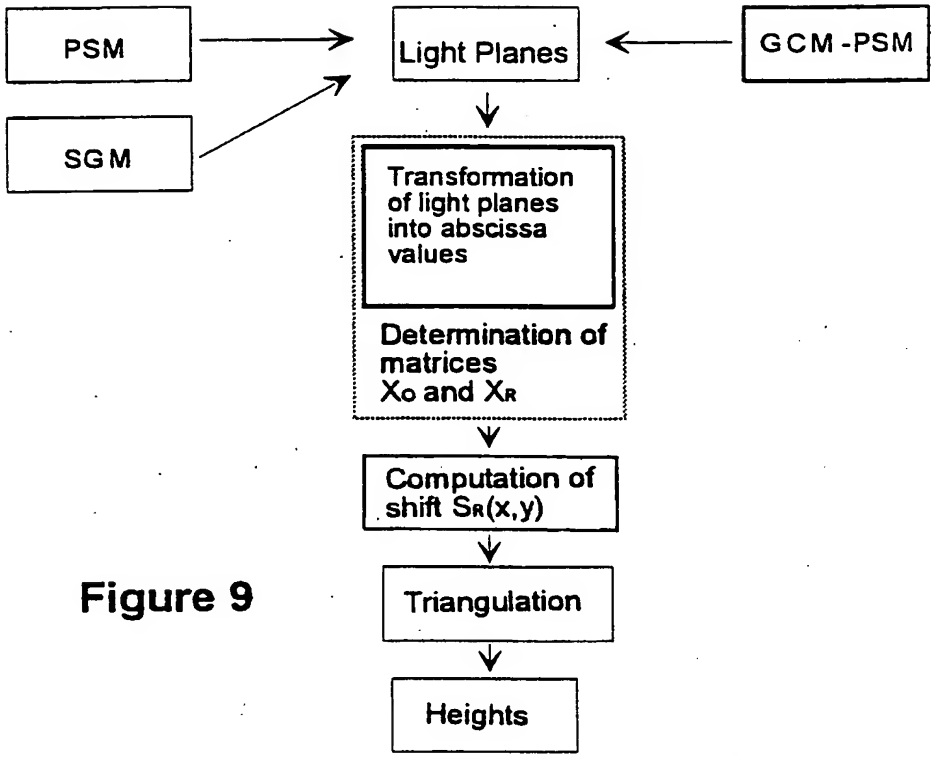

Figure 9

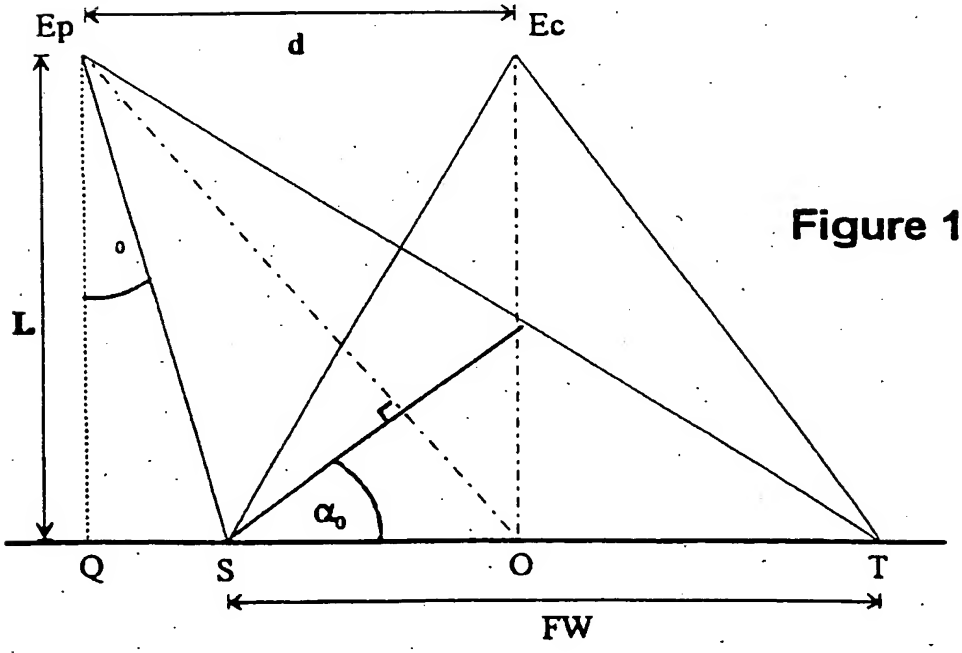

Figure 10

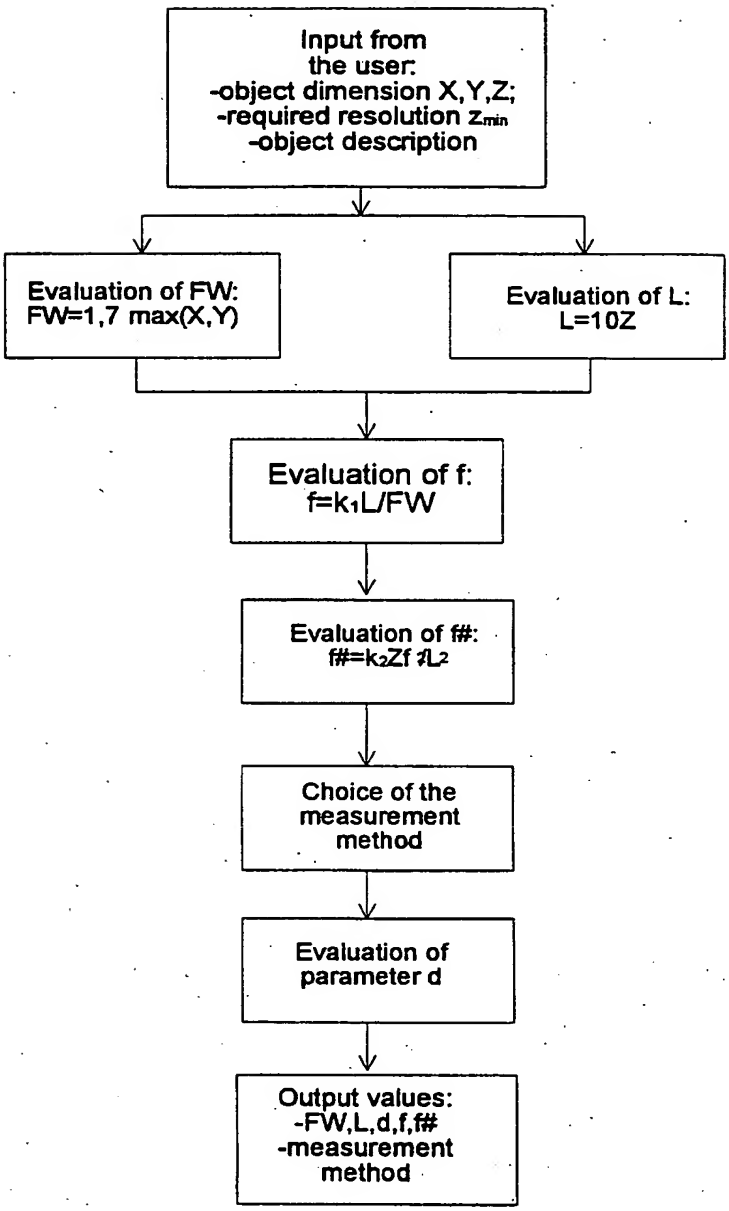
Input from the user: -object dimension X,Y,Z; -required resolution z_{min} -object description
Evaluation of FW: FW=1,7 max(X,Y)
Evaluation of L: L=10Z
Evaluation of f: $f=k_1L/FW$
Evaluation of f#: $f\#=k_2Zf/L^2$
Choice of the measurement method
Evaluation of parameter d
Output values: -FW,L,d,f,f# -measurement method

Figure 11.

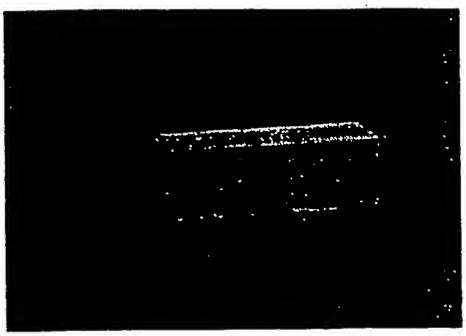

fig.12a

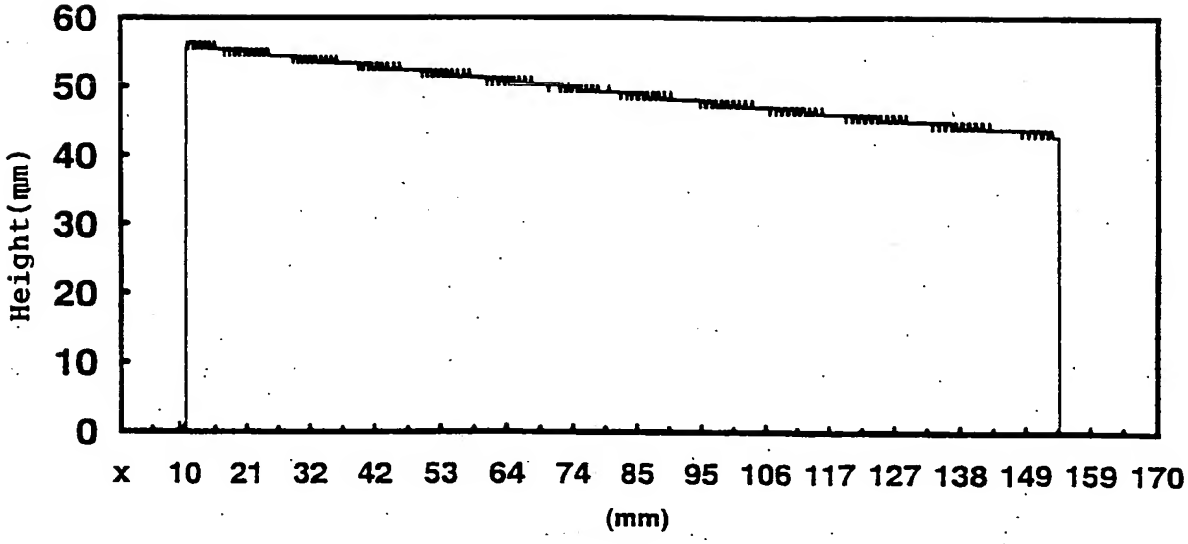

fig.12b

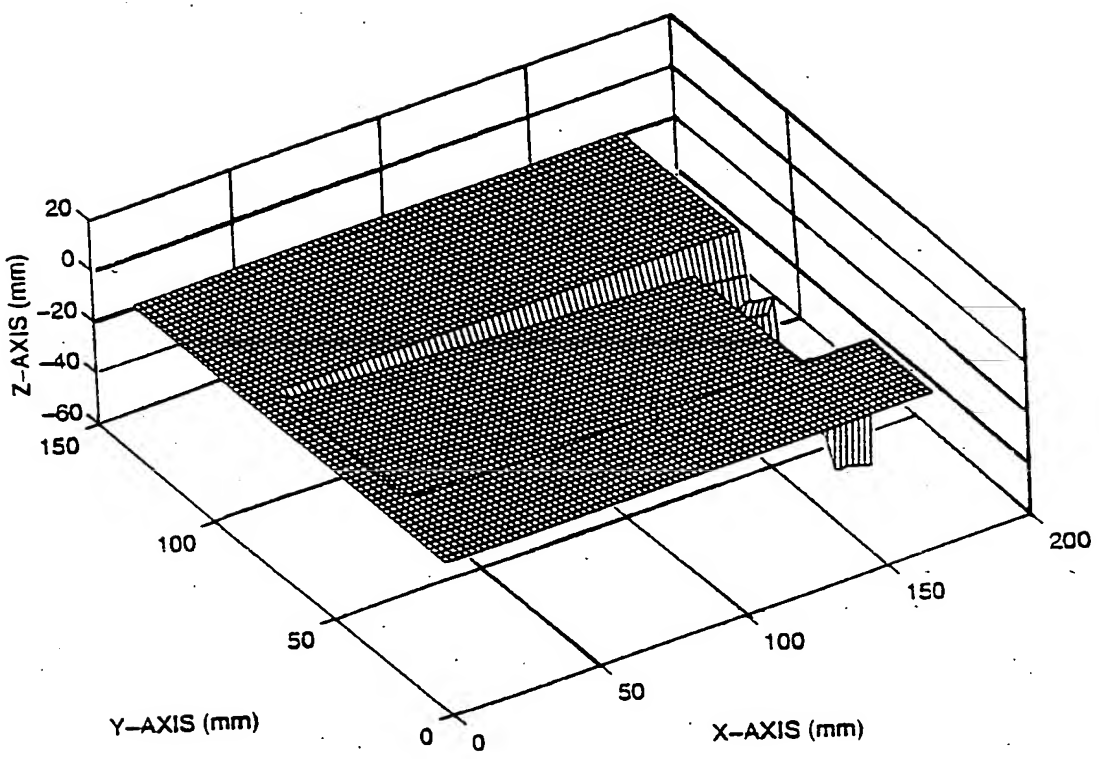
20
0
-20
-40
-60
Z-AXIS (mm)
150
100
50
0
Y-AXIS (mm)
0
50
100
150
200
X-AXIS (mm)

fig.13

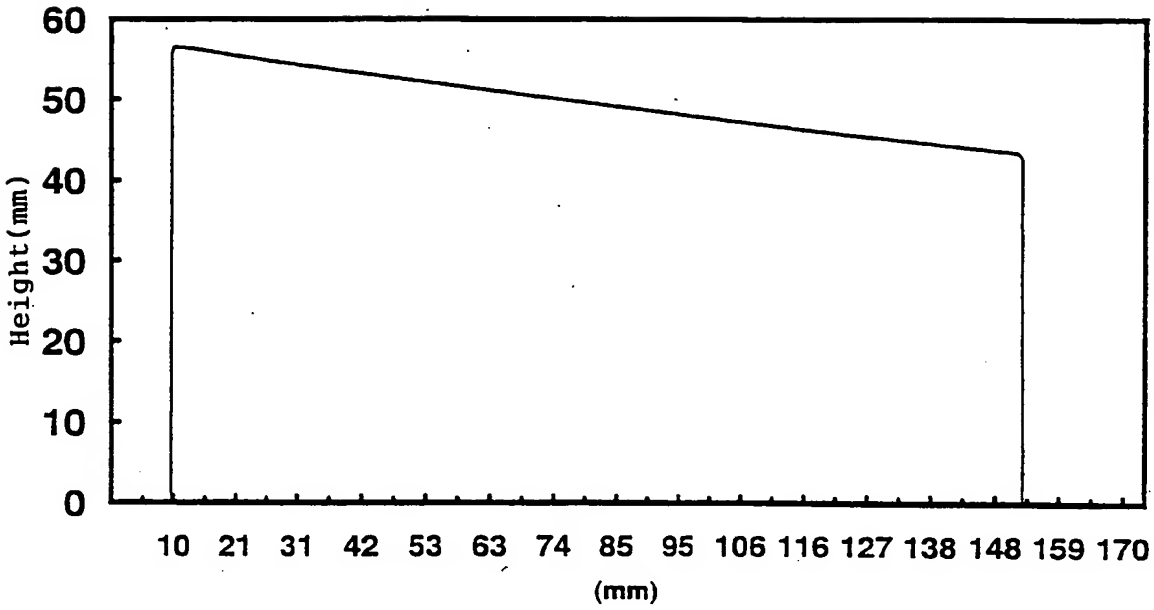
60
50
40
30
20
10
0
Height(mm)
10 21 31 42 53 63 74 85 95 106 116 127 138 148 159 170
(mm)

fig.14

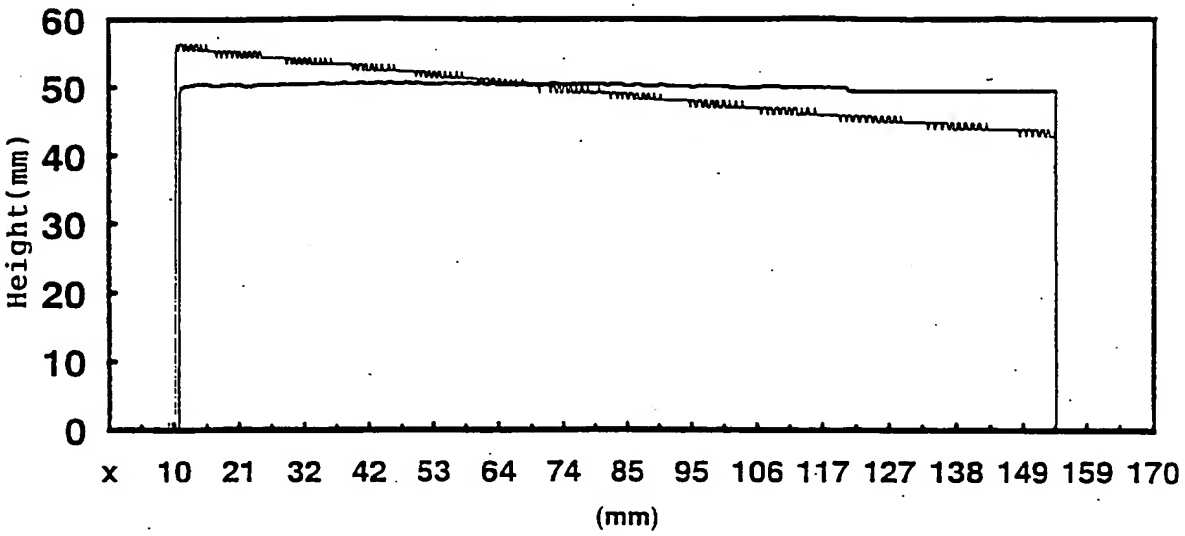
60
50
40
30
20
10
0
Height(mm)
x 10 21 32 42 53 64 74 85 95 106 117 127 138 149 159 170
(mm)

fig.15

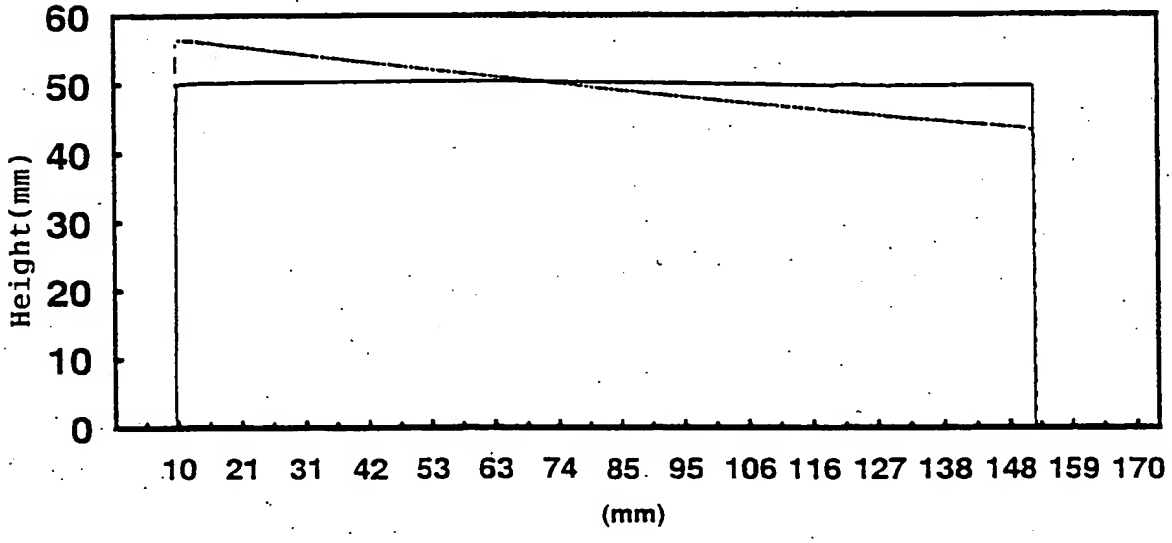
60
50
40
30
20
10
0
Height(mm)
10 21 31 42 53 63 74 85 95 106 116 127 138 148 159 170
(mm)

fig.16

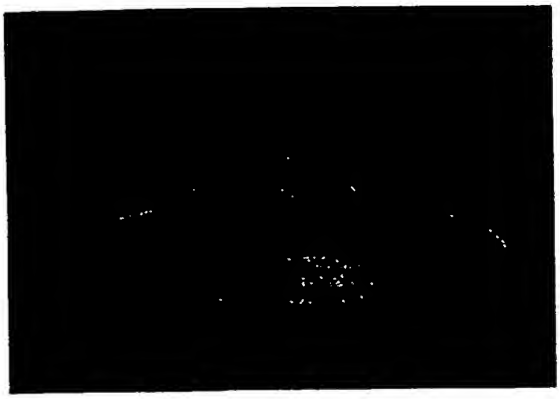

fig.17a

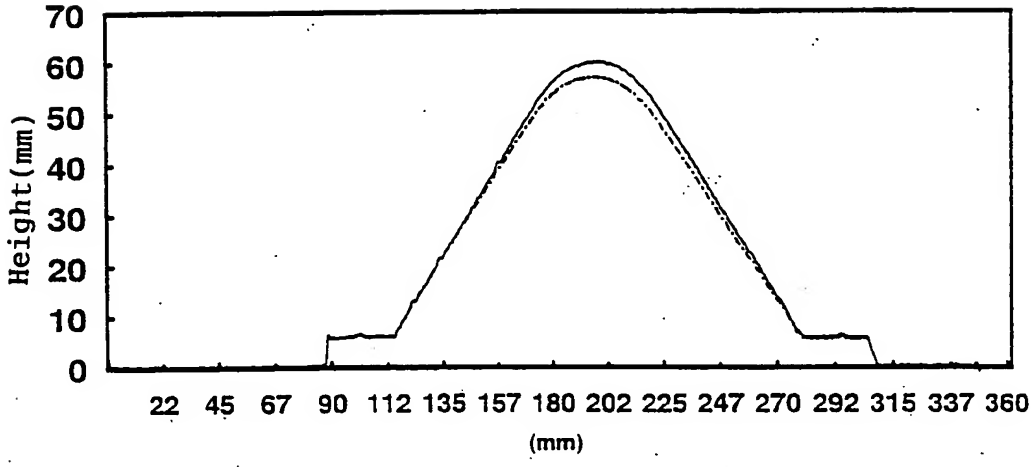

fig.17b

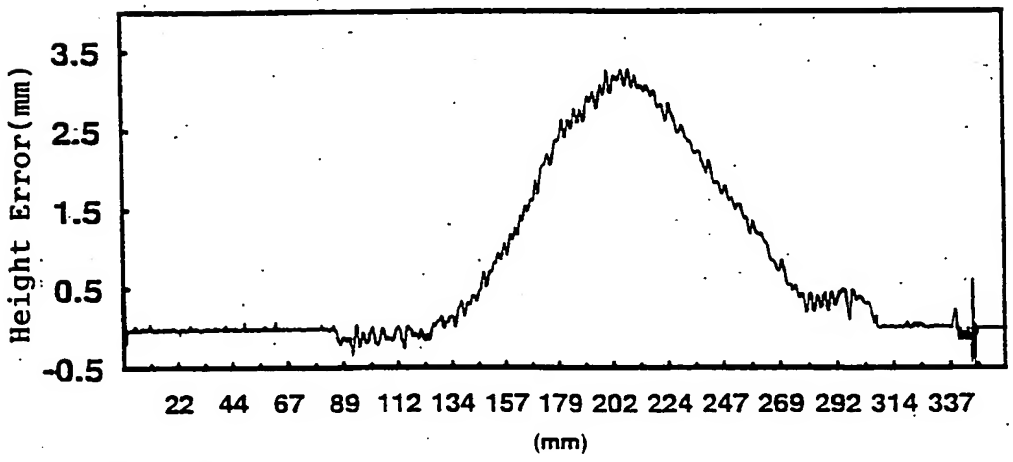

fig.17c

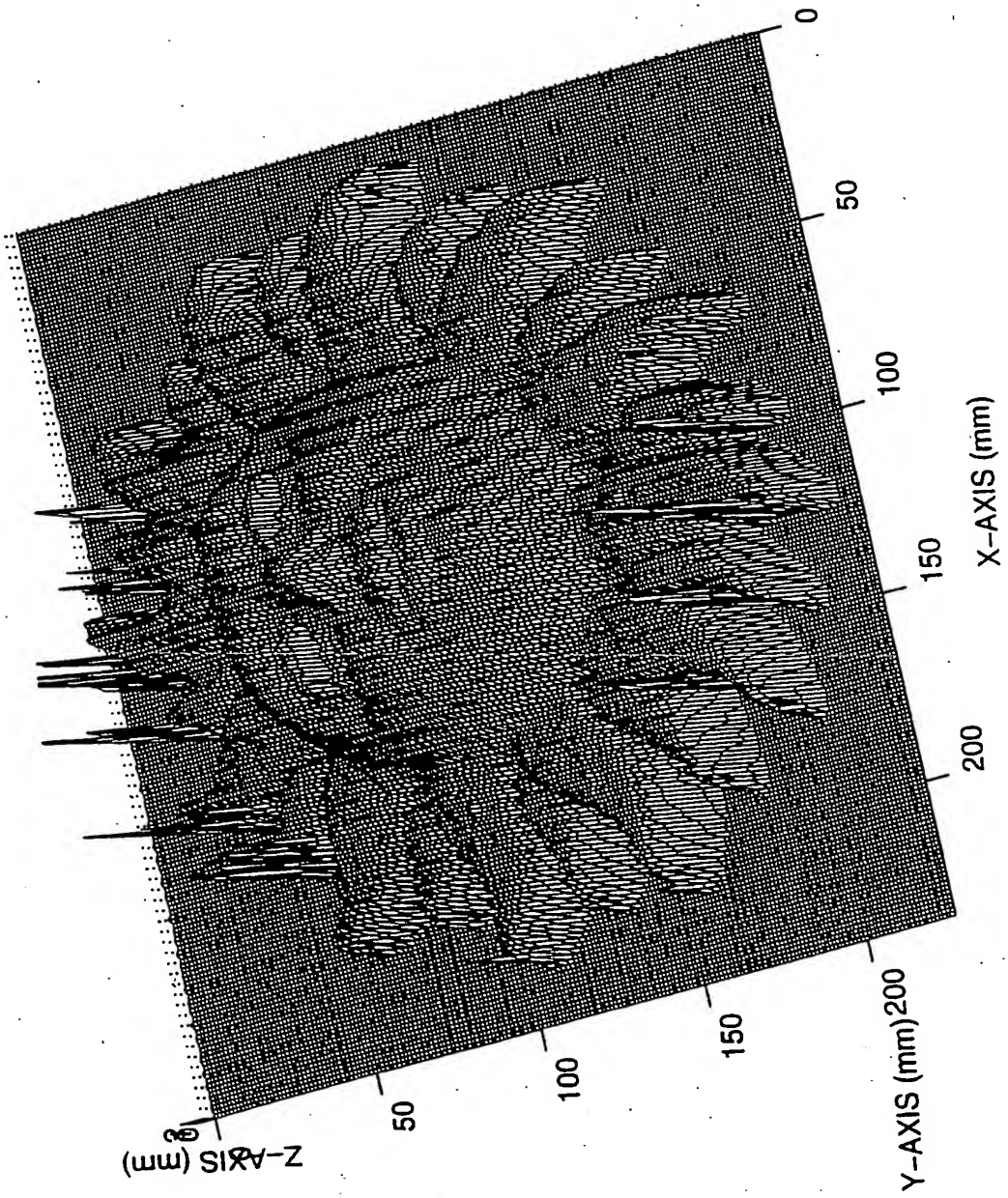

fig.18a

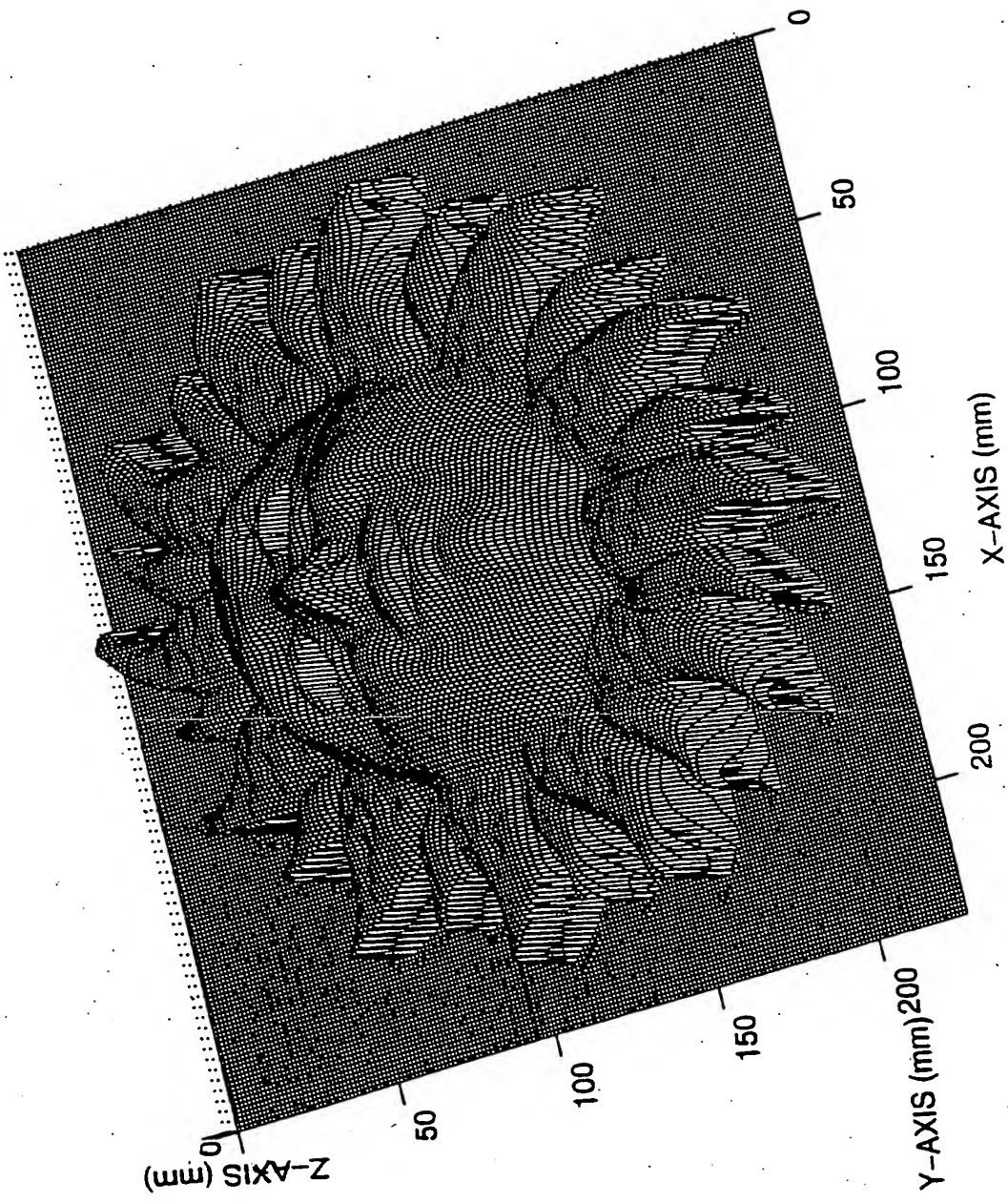

fig.18b

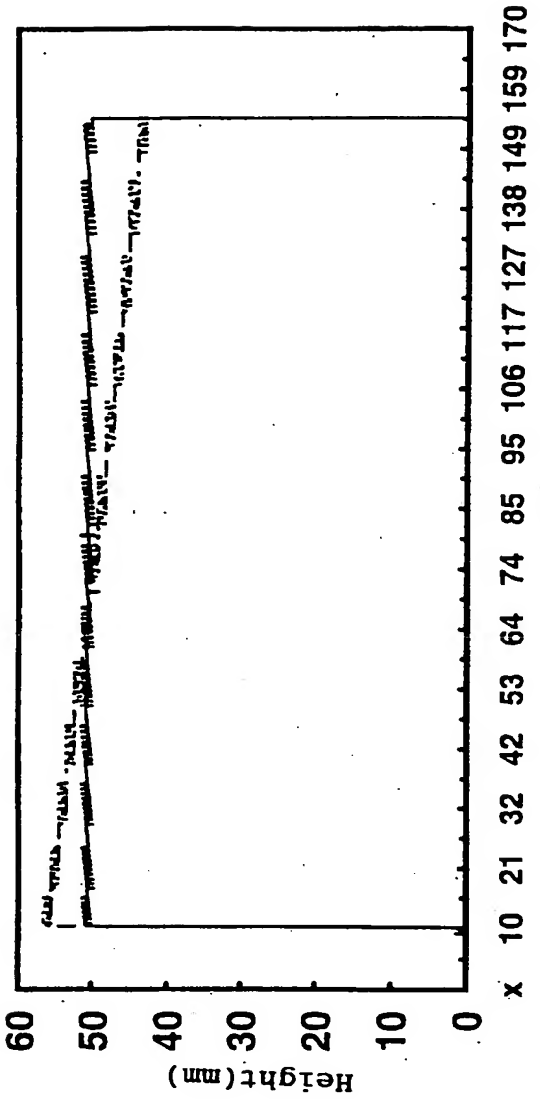
Height(mm)
60
50
40
30
20
10
0
x 10 21 32 42 53 64 74 85 95 106 117 127 138 149 159 170
(mm)

fig.19

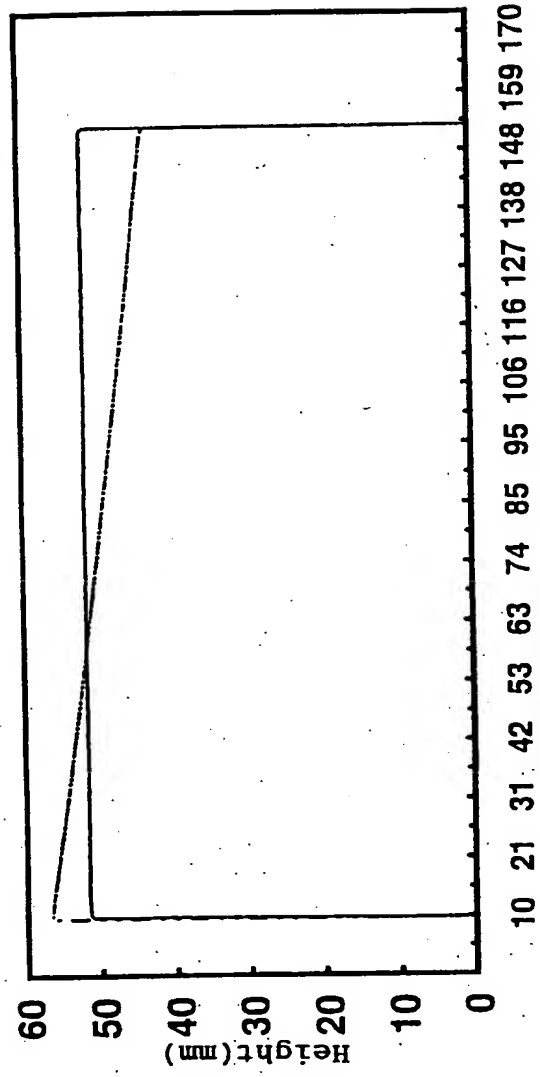
Height(mm)
60
50
40
30
20
10
0
10 21 31 42 53 63 74 85 95 106 116 127 138 148 159 170
(mm)

fig.20

16/16

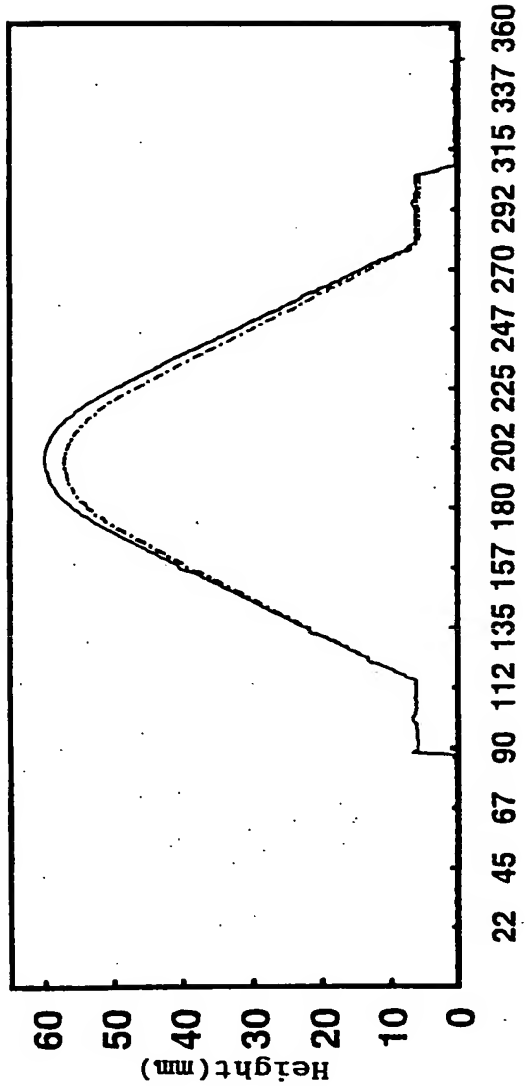
Height(mm)
60
50
40
30
20
10
0
22 45 67 90 112 135 157 180 202 225 247 270 292 315 337 360
(mm)

fig.21

INTERNATIONAL SEARCH REPORT

International Application No
PCT/EP 98/07705

A. CLASSIFICATION OF SUBJECT MATTER
IPC 6 G01B11/24

According to International Patent Classification (IPC) or to both national classification and IPC

B. FIELDS SEARCHED

Minimum documentation searched (classification system followed by classification symbols)
IPC 6 G01B

Documentation searched other than minimum documentation to the extent that such documents are included in the fields searched

Electronic data base consulted during the international search (name of data base and, where practical, search terms used)

C. DOCUMENTS CONSIDERED TO BE RELEVANT

Category °	Citation of document, with indication, where appropriate, of the relevant passages	Relevant to claim No.
A	DE 195 15 949 A (CONTINENTAL AG) 14 November 1996 see the whole document	1
A	WO 96 12160 A (MOORE JOHN HUMPHREY) 25 April 1996 see page 23, line 1 - line 19; figures 1,2	1
A	US 5 612 786 A (HUBER EDWARD D ET AL) 18 March 1997 see column 2, line 39 - line 52; figure 1	1

☐ Further documents are listed in the continuation of box C.

☒ Patent family members are listed in annex.

° Special categories of cited documents :

"A" document defining the general state of the art which is not considered to be of particular relevance

"E" earlier document but published on or after the international filing date

"L" document which may throw doubts on priority claim(s) or which is cited to establish the publication date of another citation or other special reason (as specified)

"O" document referring to an oral disclosure, use, exhibition or other means

"P" document published prior to the international filing date but later than the priority date claimed

"T" later document published after the international filing date or priority date and not in conflict with the application but cited to understand the principle or theory underlying the invention

"X" document of particular relevance; the claimed invention cannot be considered novel or cannot be considered to involve an inventive step when the document is taken alone

"Y" document of particular relevance; the claimed invention cannot be considered to involve an inventive step when the document is combined with one or more other such documents, such combination being obvious to a person skilled in the art.

"&" document member of the same patent family

Date of the actual completion of the international search	Date of mailing of the international search report
8 March 1999	15/03/1999

Name and mailing address of the ISA	Authorized officer
European Patent Office, P.B. 5818 Patentlaan 2 NL - 2280 HV Rijswijk Tel. (+31-70) 340-2040, Tx. 31 651 epo nl, Fax: (+31-70) 340-3016	Vorropoulos, G

Form PCT/ISA/210 (second sheet) (July 1992)

INTERNATIONAL SEARCH REPORT

Information on patent family members

Ir tional Application No
PCT/EP 98/07705

Patent document cited in search report	Publication date	Patent family member(s)	Publication date
DE 19515949 A	14-11-1996	NONE	
WO 9612160 A	25-04-1996	AU 3702295 A	06-05-1996
		EP 0786072 A	30-07-1997
US 5612786 A	18-03-1997	US 5561526 A	01-10-1996
		US 5557410 A	17-09-1996